NUMERICAL STUDY OF THE ONSET OF CONVECTION WITH A NET FLOW OF FLUID THROUGH POROUS MEDIA HEATED FROM BELOW

by

Ramadan A. Mohamed

ProQuest LLC.
789 East Eisenhower Parkway
P.O. Box 1346
Ann Arbor, MI 48106 – 1346

T-2603

A thesis submitted to the faculty and the Board of Trustees of the Colorado School of Mines in partial fulfillment of the requirements for the degree of Master of Science (Chemical and Petroleum-Refining Engineering).

Golden, Colorado

Date MARCH 17, 1982

Signed: _____
Ramadan A. Mohamed

Approved: _____
Michael C. Jones
Thesis Advisor

Golden, Colorado

Date MARCH 17, 1982

_____
Philip F. Dickson-Profess
and Head, Chemical and
Petroleum-Refining Engine
ering

بسم الله الرحمن الرحيم

IN THE NAME OF GOD
MOST COMPASSIONATE AND MERCIFUL

ABSTRACT

A numerical study is made of the problem of two dimensional transient natural convection of fluid flow through porous media heated from below. The system is taken to be initially at a uniform temperature. The system is heated from below considering the side walls to be perfectly insulated.

The problem is formulated in terms of three simultaneous partial differential equations, (a) a time dependent equation in temperature, (b) an elliptic equation relating stream function and vorticity, (c) a time dependent equation in vorticity. Several procedures involving various finite difference approximations of these equations are used and an investigation is made into the stability of of such methods. The explicit up-wind difference technique is employed to advance the fields of temperature and vorticity across a time step from suitable difference forms of equations (a & c). The method of successive over-relaxation is then used to solve equation (b) for new values of stream function, from which new velocity fields are obtained.

The criterion for the onset of convection is found to be in an excellent agreement with the previous investigations, for the non-flow case, that is the critical Darcy-Rayleigh number $(Ra \frac{K}{H^2}) \simeq 4\pi^2$. For the flow case a straight line

is found when critical Darcy-Rayleigh numbers are plotted against Reynolds numbers. The region above the line is considered to be unstable, while the region under it is the stable one.

Solutions were found for Grashof numbers ranging from 9.33×10^{1} to 2.18×10^{15}, for dimensionless inverse permeability from 0.0 to 4×10^{11}, for Reynolds numbers from 0.0 to 100, for Prandtl number of 0.733, for volumetric specific heat ratio of $2. \times 10^{-4}$ and for aspect ratios of 0.5, 1.0 and 2.0. The results are presented as transient and steady state plots of streamlines and isotherms.

As a practical application, the stability of vertical flow oil shale retorts was considered. For typical operating parameters, these appear to be stable.

TABLE OF CONTENTS

LIST OF FIGURES

LIST OF TABLES

ACKNOWLEDGMENT

The author wishes to express his deep sense of gratitude to Dr. M. C. Jones for suggesting this thesis topic, his guidance, and his encouragement throughout the course of this work.

Grateful appreciation to Dr. Philip F. Dickson and Dr. V. F. Yesavage for serving as committee members. In addition, the author is indebted to the Libyan people for their support.

Finally I would like to give a very special thanks to my parents and my brothers who are always proud of me and give in every way they can to support me; and thanks to my wife for her patience, continued encouragement and unselfish love throughout this work.

CHAPTER I

INTRODUCTION

1.1 Objective

The purpose of this work was to investigate heat convection with respect to stability in porous media with net flow of the working fluid and subjected to a vertical temperature gradient imposed by heating from below.

The objective was to find a criterion for the onset of convection. The investigation was carried out numerically by solving the system of partial differential equations considered to describe two dimensional fluid flow in porous media (continuity, momentum and energy). The system of partial differential equations was solved under the assumptions of constant physical properties of the working fluid, and using the Boussinesq approximation for the density, that,for small temperature variations, the density can be considered constant everywhere except in the buoyant force term.

This problem is of some practical interest, especially in oil shale retorts, where the cold incoming air flows in above the combustion zone, and is therefore potentially convectively unstable in the rock matrix.

1.2 Literature Review and General Discussion of Natural Convection

When a horizontal layer of fluid is being heated from below in a gravitational field, the possibility exists that convection currents arise, due to the density gradient. In the case where the temperature gradient exceeds a certain critical value, the fluid state becomes unstable because the buoyant force is sufficient to overcome the dissipative effects. This phenomenon was first observed by Bénard in 1900 (1). The buoyant force can also be produced by internal heating. The ratio of restraining viscous force and the buoyant force tending to drive the convection is defined as Rayleigh number.

$$Ra = \frac{\beta g \Delta T H^3}{\alpha \nu}$$

where ΔT is the temperature difference across the layer, H is the depth of the fluid layer, β, ν, α are respectively the volumetric expansion coefficient, kinematic viscosity, and thermal diffusivity of the fluid, g is the acceleration of gravity.

Rayleigh (2) made the first theoretical analysis of the so-called Bénard problem concerning the stability of a fluid layer in the presence of a temperature gradient parallel to the gravitational force. He used linear theory to analyze the instability problem.

Following Bénard's classical experiments, both physical and mathematical explanations have been pursued by many outstanding scientists. Pellew and Southwell (3) performed a linear stability analysis of a viscous fluid layer heated from below under a variety of boundary conditions and found that convection resulting from instability of the conduction solution could occur with a variety of cell shapes can be achieved by using non-linear analysis. Malkus and Veronis (4) introduced the idea of finite amplitude thermal convection and found the possibility of additional transitions in the nature of heat transfer beyond the first transition from conduction convection. Following this finite amplitude disturbance concept, Schluter, Lortz and Busse (5) found that two-dimensional rolls are a possible form of convection.

In addition to the theoretical work, many experimental efforts has been devoted to determining the heat transfer relationship and convective transitions for Benard convection. Some early studies are those of Schmit and Milverson (6), Malkus (7), and Krishnamurti (8) made detailed measurements of the heat transfer relationship. Rossby (9) performed the experiment to study Benard convection including the rotation effect.

Convection with an internal heating source drew interest in the past two decades. Buoyant forces in this case are driven by a non-linear conduction temperature field. Uniform internal heating has been proposed as a model for the earth's mantle (10) and outer regions of steller interiors (11). The Rayleigh number for this problem is defined as

$$Ra = \frac{\beta g H^3}{\nu \alpha}\left(\frac{SH^2}{2k}\right)$$

Here temperature difference across the layer in conduction is $\Delta T = (SH^2/2k)$, where S is the internal heat source strength and k is the thermal conductivity of the fluid. This parameter is always meaningful for any bounding temperature.

Goldstein, Sparrow and Jonsson (12) studied the linear stability problem for an internally heated fluid layer. They found that with increasing departure from the linear temperature profile, the fluid layer becomes more prone to instability, that is, the critical Rayleigh number decreases. Roberts (13) made linear stability calculations for an internally heated fluid layer with an insulated lower boundary. Thrilby (14) extended Roberts work with a numerical study. An experimental investigation of the same problem was carried out by Tritton and Zarraga (15). Their study, largely qualitative, involved visualization

of the flow patterns in the convection process. They found that near the critical Rayleigh number, stable hexagon cells formed with decreasing flow in the center, counter to the motion observed in Benard Convection.

In an analytical study Joseph and Shir (16) applied the "energy method" to fluid layers with uniform internal heat sources. They found that possible subcritical instabilities exist.

The stability of thermal convection in a porous medium is also an extension of Benard convection motivated by geophysical interests (3,4). In this problem flow within the porous layer is assumed to follow Darcy's Law. The Rayleigh number is modified to incorporate the permeability of the material in the layer as well as its thickness. It is defined as $Ra = \beta g \Delta T K H / \alpha_m \nu$. In this thesis we shall call this the Darcy-Rayleigh number, where K is the permeability, and α_m is the thermal diffusivity of the fluid-saturated porous layer. Analogously, another class of thermal convection to include as an extension of Benard convection is convection in a porous layer driven by density gradient produced by a uniform internal heat source. The Darcy-Rayleigh number for this case is defined the same way as for a fluid layer with internal heating, but also includes the permeability, thus,

$$Ra = \frac{\beta g K}{\alpha_m \nu} \left(\frac{SH^2}{2k_m}\right)$$

where k_m is the thermal conductivity of the fluid saturated porous layer.

Horton and Rogers (17) and Lapwood (18) show that under certain conditions, free convection may occur in a fluid saturated porous medium uniformaly heated from below which is similar to Benard's problem. This idea has been used in studies of storage of food, in explaining the insulating problems of porous materials (19,20,21) and in seeking the solution to the problem of how to dispose of nuclear reactor water (22). It is also of interest in geophysical studies. Examples of related geophysical problems are the study of geothermal (hot spring) areas(23), earthquake (24), and volcanism (25). Schneider (26) has done experiments with horizontal porous layers heated from below and presents the heat transfer relationship in the form of Nusselt number vs Rayleigh number curves. Katto and Masuoka (27) show that by defining the thermal diffusivity as $\alpha_m = \frac{k_m}{(\rho Cp)_F}$ where k_m is the thermal conductivity of the saturated layer and

$(\rho Cp)_F$ is the density times the specific heat of saturated fluid, experimental data could be brought into better agreement with theoretical predictions for the critical Rayleigh number at which conduction first becomes unstable.

Examples of other studies are those of Elder (28). Busse and Joseph (29), using a variational method to set bounds on the heat transport for a porous layer heated from below, predict the slope of the heat transport curve (nu vs Ra_c) bo be ($1/2\ \pi^2$ at the onset of convection.

In numerical studies, there are two major numerical methods that have been applied to the problem of a porous medium heated from below. Most common are the finite difference techniques, used typically by Horn (30), Horn and O'Sullivan (31), Catagirone (32), Holst and Aziz (33), Cheng and Teckchandani (34), and Rana, Horn and Cheng (35). The techniques vary from study to study, but generally consist of the solution of an elliptic Poisson-type equation derived from conservation of mass and momentum together with the time dependent, hyperbolic convervation of energy equation. The energy equation is commonly solved using explicit or iterative time differencing, and the Poisson flow equation either by direct solution using even and odd reduction, for example, Horne and O'sullivan (31) or iteratively by alternating implicit difference methods, for example Catagirone (32), Wilks(36).

The second method is to use spectral decomposition, which was used by Strous (37), Strous and Schubert (38) and Horne(30). In this technique the temperature field is expressed in terms of Fourier modes. Thus the partial differential set of equations is reduced to a set of simultaneous nonlinear ordinary differential equations in terms of Fourier temperature components.

We have been unable to find any reported theoretical or experimental studies for the convective instability of fluid saturated porous media heated from below with net flow of the fluid. This directly leads to the problem at hand.

CHAPTER II

DEVELOPMENT OF GOVERNING EQUATIONS

2.1 Equations Governing the Problem:

Following common practice for studies of convective instability, the fluid physical properties are assumed to be constant everywhere except for the density, which is assumed to be a function of temperature in the momentum equation according to the equation of state:

$$\rho = \rho_0 / \left[1 + \beta \, (T - T_0)\right]$$

Here β is the volume expansion coefficient at T_0 and has the value of $(1/T_0)$ for the case of ideal gas. It is assumed that the applied temperature difference is small compared with $(1/\beta)$. This is the so-called Boussinesq approximation.

Thus, the fluid is considered to be incompressible, except for the term in which the variation of density is essential to the whole problem. The motion is assumed to be two dimensional.

Using the axes as shown in Figure 2.1, the governing equations (41, 40, 21, 39, 26) for the porous isotropic medium of permeability K are:

Continuity:

$$\frac{\partial u}{\partial x} + \frac{\partial v}{\partial y} = 0.0 \qquad (2.1)$$

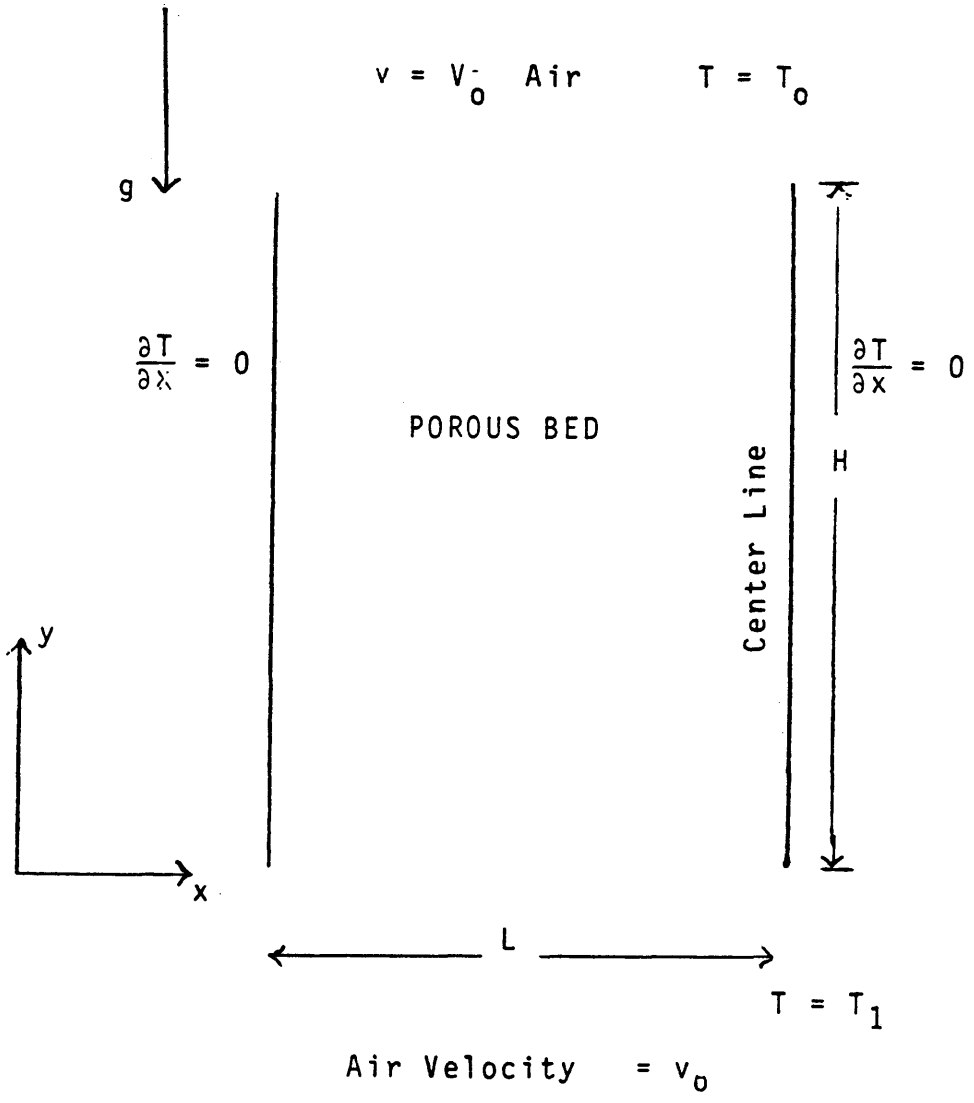

FIGURE 2.1 THE PROBLEM OF NATURAL CONVECTION OF FLUID FLOW THROUGH POROUS MEDIUM

Motion:

x - component

$$\frac{\partial u}{\partial t} + u\frac{\partial u}{\partial x} + v\frac{\partial u}{\partial y} = -\frac{1}{\rho_o}\frac{\partial p}{\partial x} + \nu\nabla^2 u - \frac{\nu}{K}u$$

y - component:

$$\frac{\partial v}{\partial t} + u\frac{\partial v}{\partial x} + v\frac{\partial v}{\partial y} = g\beta(T-T_o) - \frac{1}{\rho_o}\frac{\partial p}{\partial y} - \frac{\nu}{K}v \qquad (2.2)$$

Energy

$$\frac{\partial T}{\partial t} + (u\frac{\partial T}{\partial x} + v\frac{\partial T}{\partial y})\gamma = \frac{km}{(\rho c_p)_m}\nabla^2 T \qquad (2.3)$$

Equation (2.2) is the equation of motion using Brinkmann's extension of Darcy's Law (21). Darcy's Law is a special case resulting for low permeability, K, i.e.:

x - component

$$\frac{\partial u}{\partial t}^{0} + u\frac{\partial u}{\partial x}^{0} + v\frac{\partial u}{\partial y}^{0} = -\frac{1}{\rho_o}\frac{\partial p}{\partial x} + \nu\Delta^2 u^{0} - \frac{\nu}{K}u$$

or $\frac{\nu}{K}u = -\frac{1}{\rho_o}\frac{\partial P}{\partial x}$

y - Component

$$\frac{\nu}{K}v = g\beta(T-T_o) - \frac{1}{\rho_o}\frac{\partial p}{\partial y} \qquad (2.4)$$

For adiabatic side walls, the initial and boundary conditions are:

$t = 0$ $\quad u = v = 0,\ T = To \quad 0 \leq x \leq L, \quad 0 \leq y \leq H$

$t > 0$ $\quad u = 0,\ v = 0,\ T = To$ at $y = H$

$u = 0,\ v = 0,\ T = T_1$ at $y = 0$

$u = v = 0;\ \frac{\partial T}{\partial x} = 0$ at $x = 0$

$u = 0,\ \frac{\partial v}{\partial x} = 0,\ \frac{\partial T}{\partial x} = 0$ at $x = L$

All the above boundary conditions are for non-flow case, that is, when no fluid crosses the boundaries of the region.

For the flow case:

$t = 0, \quad u = 0, \quad v = v_o, \quad T = T_o \qquad 0 \leq x \leq L, \ o < y \leq H$

$t > 0$

$u = 0,\ v = v_o,\ T = T_o$ at $y = H$

$u = 0,\ v = v_o,\ T = T_1$ at $y = 0$

$u = 0,\ v = v_o,\ \frac{\partial T}{\partial x} = 0$ at $x = 0$

$u = 0,\ \frac{\partial v}{\partial x} = 0,\ \frac{\partial T}{\partial x} = 0$ at $x = L$

It must be noted that Darcy's Law is used for low permeability. However, for high permeability Brinkman's extension of Darcy's Law is applied, while in the limit of high permeability the Brinkman's extension of Darcy's Law reduces to the Navier-Stokes equation.

2.2 Dimensionless Form of the Equations:

Equations 2.1, 2.2, 2.3 may now be expressed in non-dimensional form by defining suitable dimensionless variables. If we define the flowing quantities as:

H : reference length

$\rho_o \frac{\mu}{H}$: reference velocity

$T_1 - T_o$: reference temperature difference

$\frac{\rho_o H^2}{\mu}$: reference time

PR : reference pressure

Then dimensionless distance, velocity, temperature, time and pressure are defined by

$$X = \frac{x}{H}, \quad Y = y/H$$

$$U = u/(\mu/\rho_o H) \quad V = v/(\mu/\rho_o H) \tag{2.5}$$

$$\theta = \frac{T-T_o}{T-T_1}, \quad \tau = t/(\rho_o H^2/\mu)$$

$$P = (p/PR)$$

From equations 2.1, 2.2, 2.3 and 2.5 the dimensionless forms of the equations of continuity, motion and energy together with the initial and boundary conditions, are now

Continuity

$$\frac{\partial U}{\partial X} + \frac{\partial V}{\partial Y} = 0 \qquad (2.6)$$

Motion

$$\frac{\partial U}{\partial \tau} + U\frac{\partial U}{\partial X} + V\frac{\partial U}{\partial Y} = \left(-\frac{H^3 PR}{\nu^2 \rho_o}\right)\frac{\partial P}{\partial X} + \nabla^2 U - N_- U \qquad (2.7)$$

$$\frac{\partial V}{\partial \tau} + U\frac{\partial V}{\partial X} + V\frac{\partial V}{\partial Y} = \left(-\frac{H^3 PR}{\nu^2 \rho_o}\right)\frac{\partial P}{\partial Y} + \nabla^2 V + Gr\theta - NV$$

Energy

$$\frac{\partial \theta}{\partial \tau} + \left(U\frac{\partial \theta}{\partial X} + V\frac{\partial \theta}{\partial Y}\right)\gamma = \frac{\gamma}{Pr}\nabla^2 \theta \qquad (2.8)$$

where the dimensionless groups appearing in the above equations can be defined as

$N = H^2/k$, a dimensionless reciprocal permeability

$Pr = \frac{\mu Cp}{km}$, the Prnadtl number

$\gamma = (\rho Cp)f/(\rho Cp)m$, a heat capacity ratio

$Gr = \frac{g\beta(T-T_1)}{\nu^2} H^3$, the Grashof number

Initial and Boundary Conditions

For Non Flow Case:

$\tau = 0 \quad U = V = 0, \quad \theta = 0 \quad 0 \leq X \leq L/H, \quad 0 \leq Y \leq 1$

$\tau > 0$

$$U = 0,\ V = 0,\ \theta = 0 \quad \text{at } Y = 1$$

$$U = 0,\ V = 0,\ \theta = 1.0 \quad \text{at } Y = 0$$

$$U = V = 0,\ \frac{\partial \theta}{\partial X} = 0 \quad X = 0$$

$$U = 0,\ \frac{\partial V}{\partial X} = 0,\ \frac{\partial \Theta}{\partial X} = 0 \quad \text{at } X = L/H$$

and for the flow case (down flow)

$\tau = 0 \quad U = 0, \quad V = -Re, \quad \theta = 0, \quad 0 \leq X \leq L/H, \quad 0 \leq Y \leq 1$

$\tau > 0$

$$U = 0,\ V = -Re,\ \theta = 0 \quad \text{at } Y = 1$$

$$U = 0,\ V = -Re,\ \theta = 1.0 \quad \text{at } Y = 0$$

$$U = 0,\ V = -Re,\ \frac{\partial \theta}{\partial X} = 0 \text{ For } X = 0 \text{ and}$$

$$U = 0,\ \frac{\partial \Theta}{\partial X},\ \frac{\partial V}{\partial X} = 0 \text{ For } X = L/H$$

where

$$Re = \frac{\rho v_o H}{\mu} = \text{Reynolds Number}$$

2.3 Elimination of Pressure from Equation of Motion: Introduction of Stream Function and Vorticity

Equation (2.7) does not represent a form entirely suited to finite difference computation, owing to the appearance of pressure in both equations of motion. An equivalent, but more convenient version of (2.7) will now be derived. Again following a common procedure, let the X and Y- momentum balances be differentiated with respect to Y and X respectively, and let either of resulting equations be subtracted from the other. Since $\frac{\partial^2 P}{\partial X \partial Y} = \frac{\partial^2 P}{\partial Y \partial X}$, pressure is eliminated; also, the continuity relation $\frac{\partial U}{\partial X} + \frac{\partial V}{\partial Y} = 0$ causes certain other terms to vanish and there results.

$$\frac{\partial}{\partial \tau}\left(\frac{\partial U}{\partial Y} - \frac{\partial V}{\partial X}\right) + U\left(\frac{\partial^2 U}{\partial X \partial Y} - \frac{\partial^2 V}{\partial X^2}\right) + V\left(\frac{\partial^2 U}{\partial Y^2} - \frac{\partial^2 V}{\partial X \partial Y}\right) +$$

$$\left(\frac{\partial U}{\partial X}\frac{\partial U}{\partial Y} - \frac{\partial U}{\partial X}\frac{\partial V}{\partial X}\right) + \left(\frac{\partial V}{\partial Y}\frac{\partial U}{\partial Y} - \frac{\partial V}{\partial Y}\frac{\partial V}{\partial X}\right) = \frac{\partial^3 U}{\partial X^2 \partial Y} - \frac{\partial^3 V}{\partial X^3} +$$

$$\frac{\partial^3 U}{\partial Y^3} - \frac{\partial^3 V}{\partial Y^2 \partial X} - N\left(\frac{\partial U}{\partial Y} - \frac{\partial V}{\partial X}\right) - Gr\frac{\partial \theta}{\partial X} \qquad (2.9)$$

The solenoidal flow implied by the continuity equations guarantees the existence of a dimensionless stream function, ψ, such that

$$U = \frac{\partial \psi}{\partial Y} , \qquad V = - \frac{\partial \psi}{\partial X} \tag{2.10}$$

The vorticity ξ is defined as

$$\xi = \nabla \times \vec{V}$$

It can be shown that the dimensionless vorticity is

$$w = - \left(\frac{\partial U}{\partial Y} - \frac{\partial V}{\partial X} \right)$$

Equation (2.9) then can be written as

$$\frac{\partial w}{\partial \tau} + U \frac{\partial w}{\partial X} + V \frac{\partial w}{\partial Y} = Gr \frac{\partial \theta}{\partial X} - N\, w + \nabla^2 w \tag{2.11}$$

When equation (2.4) is expressed in non-dimensional form, by following the same procedures as were followed for the case of Brinkman's extension of Darcy's Law, the resulting equation will be,

$$w = \frac{Gr}{N} \left(\frac{\partial \theta}{\partial X} \right) \tag{2.12}$$

The initial and boundary conditions are,

For the non-flow case:

$\tau = 0$ $\quad w = 0 \quad \theta = 0$

$\quad V = 0 \quad U = 0$ } For $0 \leq X \leq L/H$, $0 \leq Y \leq 1$

$\quad \psi = 0$

$\tau > 0$ $\quad \psi = V = U = 0$ at $Y = 1.0$ and $Y = 0.0$

$\quad \theta = 0$ at $Y = 1.0$

$\quad \Theta = 1.0$ at $Y = 0.0$

$$\psi = U = V = 0, \frac{\partial \theta}{\partial X} = 0 \qquad \text{at } X = 0$$

$$U = 0, \frac{\partial V}{\partial X} = 0 \quad \frac{\partial \theta}{\partial X} = 0 \quad \text{at } X = L/H$$

and for the downflow case

$\tau = 0$ $W = 0$, $\theta = 0$ For $0 \leq X \leq L/H$, $0 \leq Y \leq 1$

$V = -Re$, $U = 0$

$\tau > 0$ $\psi = ReX - C$ $U = 0$, $V = -Re$ at $Y = 0$ and $Y = 1$

$\theta = 0$ at $Y = 1$

$\theta = 1.0$ at $Y = 0$

$U = 0$, $V = -Re$, $\frac{\partial \theta}{\partial X} = 0$ at $X = 0$

$U = 0$, $\frac{\partial V}{\partial X} = 0, \partial\theta/\partial X = 0$ at $X = L/H$

For more details on boundary conditions see section 3.5.

CHAPTER III
METHOD OF SOLUTION

3.1 Introduction

The partial differential equations (P.D.Es) governing the problem have been established as

$$\frac{\partial w}{\partial \tau} + U \frac{\partial w}{\partial X} + V \frac{\partial w}{\partial Y} = Gr \frac{\partial \theta}{\partial X} + \nabla^2 w - N w \qquad (3.1)$$

$$\frac{\partial \theta}{\partial \tau} + \left(U \frac{\partial \theta}{\partial X} + V \frac{\partial \theta}{\partial Y}\right) \gamma = \frac{\gamma}{Pr} \nabla^2 \theta \qquad (3.2)$$

$$w = - \nabla^2 \psi \qquad (3.3)$$

where $\gamma = (\rho Cp)_f / (\rho Cp)_m$

plus associated initial and boundary conditions and two relations between stream function and velocities. Equations (3.1) and (3.2) relate the first order time derivatives, whereas equation (3.3) states that the Laplacian of the stream function equals minus the vorticity, and contains no derivatives involving time. The vorticity and energy equations are classed as of parabolic type. Unfortunately, they are non-linear due to the presence of the coefficient velocites U and V. On the other hand, the stream function/vorticity relation is an elliptic type.

Briefly, equations (3.1), (3.2) and (3.3) will be represented in finite difference form. The difference of (3.1) and (3.2) may then be used to predict the changes of temperature and vorticity across a time step. Solution of the difference form of (3.3) then yields a new stream function. This procedure may be repeated for as many time steps as desired.

The methods available for obtaining a finite difference approximation (F.D.A) to the solution of parabolic and elliptic (P.D. Es) differ in certain features and so the two types will be treated in turn in sections (3.3) and (3.4).

3.2 System of Grid Points

It is first to establish a system of grid points in the region occupied by the independent variables in obtaining the (F.D.A) to the solution of any (P.D.Es). The scheme is known as a rectangular grid, shown in (Fig. 3.1). Square meshes of size h x h are chosen for the numerical work. Because of the symmetry about the centerline only half of the flow needs to be computed, thus resulting in large savings in computational efforts.

The subscripts (i,j) denote the point having space coordinates $X = (i-1)\Delta X = (j-1)\Delta X$. In addition, the third subscript could be used to denote the number of time

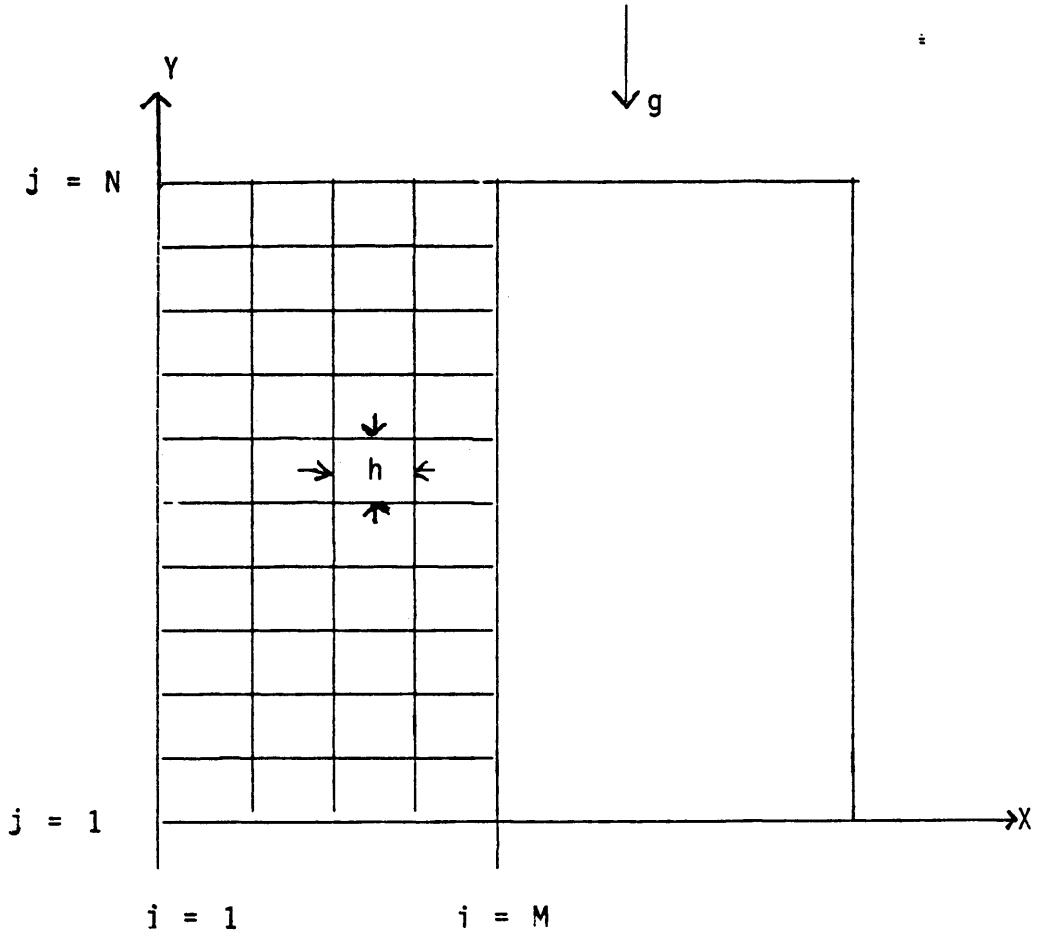

FIGURE 3.1 SYSTEM OF GRID POINTS

increments $\Delta\tau$ elapsed since $\tau = 0$. Now a three-dimensional array can easily occupy a large amount of computer storage. Also, the computations in this work involve values only one time step removed from the 'current'value of time. Hence, instead of working with (e.g.) the three-dimensional array $\theta_{i,j,n}$, where the subscript n denotes a value of temperature θ at time $\tau = n\Delta\tau$, it is here thought preferable to employ instead two-dimensional array, such as $(\theta_{i,j})$, and $(\theta'_{i,j})$, where $(\theta'_{i,j})$ denotes a value just one time step ahead of $(\theta_{i,j})$. As soon as the new values of $\theta'_{i,j}$ at the end of a particular time step are computed, they then become the starting values $\theta_{i,j}$ for the next time increment, and so the computation proceeds.

3.3 Difference Form of Stream Function/Vorticity Equation

The methods of obtaining (F.D.A) to elliptic type (P.D.E.) are well established. The Laplacian is approximated by central difference.

$$\frac{\psi_{i-1,j} - 2\psi_{i,j} + \psi_{i+1,j}}{\Delta X^2} +$$

$$\frac{\psi_{i,j-1} - 2\psi_{i,j} + \psi_{i,j+1}}{\Delta Y^2} = -w_{i,j} \qquad (3.4)$$

For $\Delta X = \Delta Y = h$

Equation (3.4) can be written as

$$\psi_{i,j} = \frac{1}{4}(\psi_{i-1,j} + \psi_{i+1,j} + \psi_{i,j-1} + \psi_{i,j+1}) - \frac{h^2}{4} w_{i,j} \qquad (3.5)$$

An improved technique, called successive overrelaxation (S.O.R) method, gives faster convergence. This method used the following iteration scheme for a rectangular domain of square meshes. Suppose that the field of vorticity is already known together with an estimate $\psi^{(n)}_{i,j}$ of the stream function at every point after the nth iteration. Then a new estimate $\psi^{(n+1)}_{i,j}$ is

$$\psi^{(n+1)}_{i,j} = \psi^{(n)}_{i,j} + \frac{\omega}{4}(\psi^{(n+1)}_{i-1,j} + \psi^{(n)}_{i+1,j} + \psi^{(n+1)}_{i,j-1} + \psi^{(n)}_{i,j+1} - 4\psi^{(n)}_{i,j} - h^2 w_{i,j}) \qquad (3.6)$$

Where (ω) is an arbitrary iteration parameter. If ω = 1.0, successive overrelaxation is equivalent to the Gauss-Seidel method. As (ω) is increased beyond unity, the number of iterations required to produce, in some sense, a given degree of convergence, is known to first decrease and then to increase again. The optimum value of relaxation parameter, ω_{opt}, lies between 1.0 and 2.0 (42, 43), and its exact location is a matter of some importance in reducing the amount of computation, particularly as the elliptic equation (3.3) will have to be solved repeatedly, once at every time step. The iterated results converges most rapidly when ω_{opt} is assigned the optimum value, Chow (42).

$$\omega_{opt} = \frac{8-4\sqrt{4-\alpha^2}}{\alpha^2} \qquad (3.7)$$

where α = Cos (π/M) + Cos (π/N), where M, N are, respectively, the total number of increments into which the horizontal and vertical sides of the rectangular region are divided.

3.4 Difference Form of Vorticity and Energy Equations

The procedure for treating the parabolic type (P.D.E.) may be subdivided into explicit, and implicit methods, depending on whether the space derivatives are represented at an old or at an advanced point of time. Explicit methods enable a direct calculation to be made of the values of the dependent variables at the advanced point of time; the associated computer programing tends, therefore, to be relatively simple. Although the implicit methods are generally unconditionally stable, they need more computational effort in programing.

An improved explicit method called the up-wind differencing method is used in this work. The reason for choosing this method is not only because it is simple for computer programing, but also for its advantage of handling non-linear terms appearing in the vorticity and energy equations. Furthermore, it has been proven that this method is computationally stable in the range of interest.

Chow (42) shows how the governing equations for free convection of a fluid in two-dimensional enclosure may be solved by using the up-wind differencing method. The scheme that Chow used was first developed by Torrance (44), and Torrance and Rockett (45). The method has been applied here to the porous medium equations with boundary conditions

for both zero flow across the boundaries and for a finite net flow through the medium.

The following is the up-wind difference representations of both the vorticity and the energy equations.

Vorticity:

The non-linear terms $U\frac{\partial w}{\partial X} + V\frac{\partial w}{\partial Y}$ in equation (3.1) can be approximated using the up-wind difference (40,42,43) as follows:

If we define Uf and Ub as the average velocities evaluated respectively, at half a grid forward and backward from the point (i,j), then

$$Uf = 1/2\ (U_{i+1,j} + U_{i,j})$$

$$Ub = 1/2\ (U_{i,j} + U_{i-1,j})$$

Similarly,

$$Vf = 1/2(V_{i,j+1} + V_{i,j})$$

$$Vb = 1/2(V_{i,j} + V_{i,j-1})$$

If we further define,

$$P1 = (Uf - |Uf|)\ w_{i+1,j} + (Uf + |Uf| - Ub + |Ub|)\ w_{i,j} - (Ub + |Ub|)\ w_{i-1,j} \quad (3.8)$$

$$P2 = (Vf - |Vf|)\ w_{i,j+1} + (Vf + |Vf| - Vb + |Vb|)\ w_{i,j} - (Vb + |Vb|)\ w_{i,j-1} \quad (3.9)$$

and if we let $\Delta X = \Delta Y = h$

Then $$\left(U\frac{\partial w}{\partial X}\right)_{i,j} = P1/2h \quad (3.10)$$

and

$$\left(V\frac{\partial w}{\partial Y}\right)_{i,j} = P2/2h \quad (3.11)$$

The remaining terms in (2.11) are approximated by using forward differencing in time and central differencing in space; their individual expressions follow:

$$\frac{\partial w}{\partial \tau} = \frac{w'_{i,j} - w_{i,j}}{\Delta \tau} \tag{3.12}$$

$$\frac{\partial \theta}{\partial X} = \frac{\theta_{i+1,j} - \theta_{i-1,j}}{2h} \tag{3.13}$$

Equation 3.13 can be expressed as $\frac{\partial \theta}{\partial X} = P3/2h$ (3.14)

$$\frac{\partial^2 w}{\partial X^2} + \frac{\partial^2 w}{\partial Y^2} = \frac{1}{h^2} (w_{i+1,j} - 4 w_{i,j} + w_{i-1,j} + w_{i,j+1} + w_{i,j-1}) \tag{3.15}$$

let $P4 = (w_{i+1,j} - 4w_{i,j} + w_{i-1,j} + w_{i,j+1} + w_{i,j-1})$

$$\nabla^2 w = P4/h^2 \tag{3.16}$$

Now put all terms together in the vorticity equation, and rearrange,

$$w'_{i,j} = (1-N)\, w_{i,j} + \frac{\Delta \tau}{2h} (-P1-P2+GrP3 +2P4/h) \tag{3.17}$$

Equation (2.17) can simply be approximated as

$$w'_{i,j} = \frac{Gr}{N} \left(\frac{\theta_{i+1,j} - \theta_{i-1,j}}{2h}\right) \tag{3.18}$$

Similarly, the energy equation can be approximated as:

$$\theta'_{i,j} = \frac{\Delta T}{2h} \left((-P1-P2)\gamma + \frac{2\gamma}{Pr} \frac{P4}{h}\right) \tag{3.19}$$

as θ replaces w in P1, P2 and P4.

The velocity equation (2.10) is approximated at the interior grid points using the central difference formula. The finite difference forms are:

$$V_{i,j} = -\left(\frac{\psi_{i+1,j} - \psi_{i-1,j}}{2h}\right) \tag{3.20}$$

$$U_{i,j} = \left(\frac{\psi_{i,j+1} - \psi_{i,j-1}}{2h}\right) \tag{3.21}$$

3.5 Finite Difference Form of Boundary Conditions

3.5-a Temperature

At time $\tau = 0$, the temperature distribution is such that $\theta = 0.0$ everywhere, except $\theta = 1.$ at the bottom. As time increases, the fluid temperature changes. The symmetry of the temperature field requires that,

$$\left.\frac{\partial \theta}{\partial X}\right|_{M,j} = 0 \quad \Rightarrow \theta_{M+1,j} = \theta_{M-1,j} \tag{3.22}$$

and at the boundary $X = 0$, the wall is assumed to be insulated that is

$$\left.\frac{\partial \theta}{\partial X}\right|_{1,j} = 0 \quad \Rightarrow \theta_{2,j} = \theta_{o,j} \tag{3.23}$$

The temperature along i=1 and i=M can be calculated using 3.19 with the boundary conditions (3.22) and (3.23) incorporated, that is

$$Ub = U(M-1,j)/2.$$

$$Vf = (V_{M,j+1}+V_{M,j})/2.$$

$$P1 = -2(Ub + |Ub|)\,\theta_{M-1,j} + 2\,(-Ub + |Ub|)\,\theta_{M,j}$$

$$P2 = (Vf - |Vf|)\,\theta_{M,j+1} + (Vf + |Vf| - Vb + |Vb|)\,\theta_{M,j} - (Vb + |Vb|)\,\theta_{M,j-1}$$

$$P4 = 2\theta_{M-1,j} + \theta_{M,j+1} + \theta_{M,j-1} - 4\theta_{M,j}$$

$$\theta'_{M,j} = \theta_{M,j} + \frac{\Delta\tau}{2h}\left((-P1-P2)\,\gamma + \frac{2\gamma}{Pr}\,\frac{P4}{h}\right) \tag{3.24}$$

Similarly

$$\theta'_{1,j} = \theta_{1,j} + \frac{\Delta\tau}{2h}\left((-P11 - P22)\gamma + \frac{2\gamma}{Pr}\quad P44/h\right)$$

where,

$$P11 = 2(Uf - |Uf|)\ \theta_{2,j} + 2(Uf + |Uf|)\ \theta_{1,j}$$

$$P22 = (Vf1 - |Vf1|)\ \theta_{1,j+1} + (Vf1 + |Vf1| - Vb1 + |Vb1|)\ \theta_{1,j} - (Vb1 + |Vb1|)\ \theta_{1,j-1}$$

$$P44 = 2\,\theta_{2,j} + \theta_{1,j+1} + \theta_{1,j-1} - 4\,\theta_{1,j}$$

$$Vf1 = (V_{1,j+1} + V_{1,j})/2$$

$$Vb1 = (V_{1,j-1} + V_{1,j})/2$$

3.5-b Velocity

Flow Case:

$\tau = 0 \qquad U = 0.0, \qquad V = -Re$

Where Re is the Reynolds Number to be given in the data and defined as $Re = (\rho v_0 H/\mu)$, vo is the initial fluid velocity. As time increases, U and V will be changed while at the boundaries,

$$U_{M,j} = U_{1,j} = U_{i,N} = U_{i,1} = 0.0$$

$$V_{M,j} = -\left(\frac{\psi_{M+1,j} - \psi_{M-1,j}}{2h}\right)$$

from the anit-symmetric distribution of ψ about the center line, $\psi_{M+1,j} = -\psi_{M-1,j}$

$$V_{M,j} = \frac{\psi_{M-1,j}}{h}$$

$$V_{i,1} = V_{i,N} = -Re$$

Non-Flow Case:

$\tau = 0 \qquad U = V = 0$ everywhere

$\tau > 0$ All other boundary conditions still hold as in the initial conditions

3.5 - C Stream Functions

Flow Case: (downflow)

$$\psi_{M+1,j} = - \psi_{M-1,j}$$

$$\psi_{M,j} = 0.0$$

The initial value of ψ can be derived from the relation

$$V = - \frac{\partial \psi}{\partial X} \qquad (3.25)$$

integrating (3.25) gives:

$$VX = - \psi + \psi_0; \qquad X = i\Delta X = ih$$

ψ_0 is constant and can be found as

at $i = M$ (center line) $\psi_{M,j} = 0.0$

$$Vih = - \psi_{i,j} + \psi_0$$

or $VMh = 0 + \psi_0$

if $V = - Re$

$$\psi_{i,j} = Re\ h(i-M)$$

For Non-Flow Case:

$$U = V = 0, \qquad \psi_{j,j} = 0.0$$

As time increases, the values of ψ changes, and the values of ψ at the boundaries are kept at initial values. At the center line $\psi = 0.0$

3.5-d Vorticity

$$\tau = 0 \qquad w_{i,j} = 0.0$$

As time increases, the values of w change , and the boundary values can be found as:

$$w_{i,j} = -\left(\frac{\partial^2 \psi}{\partial X^2} + \frac{\partial^2 \psi}{\partial Y^2} \right)$$

$$= \left(\frac{\partial V}{\partial X} - \frac{\partial U}{\partial Y} \right) \qquad (3.26)$$

At the boundary (1,j)

$$\left(\frac{\partial U}{\partial Y}\right)_{1,j} = 0 \quad = U_{1,j}$$

$$w_{1,j} = \left(\frac{\partial V}{\partial X}\right)_{1,j}$$

$\left(\frac{\partial V}{\partial X}\right)_{1,j}$ can be found by using three point forward difference scheme as

Take two Taylor series expansion

about the points i=1 and i=2

$$V_{2,j} = V_{1,j} + \left(\frac{\partial V}{\partial X}\right)_{1,j} h + \left(\frac{\partial^2 V}{\partial X^2}\right)_{1,j} \frac{h^2}{2!} + - - -$$

$$V_{3,j} = V_{1,j} + 2 \left(\frac{\partial V}{\partial X}\right)_{1,j} h + 4\left(\frac{\partial^2 V}{\partial X^2}\right)_{1,j} \frac{h^2}{2!} + - - -$$

Multiply the first equation by 4 and subtract the second equation from it.

$$4\ V_{2,j} - V_{3,j} = 3V_{1,j} + 2\left(\frac{\partial V}{\partial X}\right)_{1,j} h$$

or

$$\left(\frac{\partial V}{\partial X}\right)_{1,j} = \frac{4\ V_{2,j} - V_{3,j} - 3V_{1,j}}{2h}$$

$$w_{1,j} = \frac{4\ V_{2,j} - V_{3,j} - 3V_{1,j}}{2h} \tag{3.27}$$

at the center line

$$w_{M,j} = 0.0 \tag{3.28}$$

At the top and bottom boundaries

$$\left(\frac{\partial V}{\partial X}\right)_{i,1} = \left(\frac{\partial V}{\partial X}\right)_{i,N} = 0.0$$

$$U_{i,1} = U_{i,N} = 0.0$$

$$w_{i,1} = -\left(\frac{\partial U}{\partial y}\right)_{i,1}$$

by the same method as for $w_{1,j}$

$$w_{i,1} = -\left(\frac{4\ U_{i,2} - U_{i,3} - 3\ U_{i,1}}{2h}\right)$$

$$w_{i,1} = \left(U_{i,3} - 4\ U_{i,2}\right)/2h \tag{3.29}$$

$$w_{i,N} = - \left(\frac{\partial U}{\partial Y}\right)_{i,N}$$

and by taking three point backward difference scheme, the result is

$$w_{i,N} = \left(\frac{4\ U_{i,N-1} - U_{i,N-2}}{2h} \right) \qquad (3.30)$$

3.6 Procedures

The procedures to find the convection instability criterion were performed by trial and errors as follows:

1. Starting with low values, different Grashof numbers were tried for fixed values of Reynolds number and dimensionless inverse permeability. When convection currents appeared in the computer output, the values of Gr for this case and the preceeding case were recorded.
2. Values of Gr between these two values recorded in step 1 were tried until the error was minimized.
3. The average values of Gr for the highest stable and lowest unstable cases were tabulated to give the summary of runs performed.
4. Rayleigh number or Darcy-Rayleigh number are calculated from the relations

$$Ra = Gr \times Pr \quad \text{for single phase fluid}$$

$$Ra \frac{K}{H^2} = \frac{Gr \times Pr}{N} \quad \text{for porous media.}$$

5. The above procedures were repeated for other values of Re and N.

CHAPTER IV

PRESENTATION AND DISCUSSIONS OF THE RESULTS

The results presented here are divided into two sections. First the critical Rayleigh numbers are found for the case where the working fluid (air) is initially stationary (non-flow case). Then the situation where the net flow through is initially considered (flow-case). The second case is the main purpose of this work; while the first is presented for the comparison with previous investigations. In both cases, the study is performed numerically for porous media ($4\times10^{4} \leq N \leq 4\times10^{11}$), highly permeable media ($4\times10^{-2} \leq N \leq 4\times10^{-1}$) and for a single phase fluid ($0 \leq N < 4\times10^{-2}$).

Different non-dimensionless forms of the equation of motion are used accordingly. For porous media Darcy's law form is used; for highly permeable media, (eqn. 2.11), and for a single phase fluid (eqn. 2.11) is used with N = 0.0.

The results of determinations of critical Grashof and Rayleigh numbers are presented in Tables (4.2) and (4.3), and Figures (4.1) and (4.2). It is seen that solutions were found for Grashof numbers ranging from 9.33×10^{1} to 2.18×10^{15}, for N from 0.0 to 4×10^{11}, for width to height ratios of 0.5, 1. and 2., for a Prandtl number of 0.733 and for Reynolds numbers from 0.0 to 100.

Finally the flow patterns are shown in Figures (4.4-4.27) as contour plots of stream lines and iso-therms.

4.1 Non-Flow Case ($0<Re<10^{-3}$)

This section is presented here to compare with other theoretical investigations (45,46,18). The problem of the onset of convection in a porous medium has been given a conclusive answer of the same standard as in the ordinary layer of fluid. The criterion for the onset of convection currents can be derived with the governing equations in quite the same way as in a horizontal layer of fluid except that for the difference in the boundary conditions. Then the criterion, which Lapwood (18) has derived can be written as the Darcy-Rayleigh number

$$Ra. \frac{K}{H^2} = 4\pi^2$$

where Ra is the critical Rayleigh number

$$Ra = g\beta H^3 \Delta T/\nu\alpha_m$$

Table 4.1 shows the comparison between the present work and the previous investigations in computing the critical Darcy-Rayleigh number for porous and Rayleigh number for a single phase fluid.

TABLE 4.1 COMPARISON OF PRESENT WORK AND PREVIOUS INVESTIGATIONS FOR NON-FLOW CASE

	All Previous Work	Present Work	%Error
1. Porous medium (Darcey-Rayleigh No.)	$4\pi^2 = 39.48$	39.6	0.3%
2. Single Phase (Rayleigh No.)	1708	1710	0.12%

4.2 Flow Case (10^{-2} Re 100)

a. Porous Media ($4x10^4 \leq N \leq 4x10^{11}$)

Computations were made for the case of downflow of fluid (air) through porous media. The aim was to find a criterion for the onset of convection. Table (4.2) shows the variation of critical Grashof numbers as a result of changing Reynolds numbers. Figure (4.1) shows a family of straight lines when Grashof numbers are plotted vs Reynolds numbers at different values of N. Since Darcy-Rayleigh number is the most important as a criterion for the onset of convection, these numbers are plotted vs Reynolds numbers showing the lower straight line in Figure (4.3).

Figures 4.1 and 4.2 show that different values of (N) have different values of critical Grashof numbers at a fixed value of Reynolds number. However, Figure 4.3

shows that at a fixed value of Reynolds number there is only one value of critical Rayleigh number for $4 \times 10^{4} \leq N \leq 4 \times 10^{11}$ and another value for $0 \leq N \leq 4 \times 10^{-1}$.

b. Single Phase and Highly Permeable Media

The upper line of Figure (4.3) and Table (4.3) shows the criterion of the onset of convection for the highly permeable and single phase media. It must be mentioned that the region under any lines of Figure (4.3) represents the stable convection region while above it is the non-stable one.

Aspect ratios (width to height ratios) were studied and found that there were no effects on the onset of convection currents. Aspect ratios of 0.5, 1 and 2 were used in this work. Computations were made for the upflow of fluid and found that has the same convection instability criterion as for downflow.

TABLE 4.2 SUMMARY OF CRITICAL RAYLEIGH NUMBERS FOR

$4 \times 10^4 \leq N \leq 4 \times 10^{11}$

$Pr = 0.733$

$\gamma = 2.\times 10^{-4}$

Aspect Ratio = 1&2

$N = \frac{H^2}{K}$	Re	$(Gr)_c$	$(Ra)_c = \frac{Gr \times Pr}{N}$
4×10^4	0.0	2.15×10^{6}	3.94×10
	0.001	2.15×10^{6}	$3.94\times10_{2}$
	0.01	2.18×10^{7}	3.99×10^{2}
	0.1	2.18×10^{8}	3.99×10^{3}
	1.0	2.18×10^{9}	3.99×10^{4}
	10.0	2.18×10^{10}	3.99×10^{5}
	100.0	2.18×10^{11}	3.99×10^{6}
$4.\times10^{7}$	0.0	2.15×10^{9}	3.94×10
	0.001	2.15×10^{9}	$3.94\times10_{2}$
	0.01	2.17×10^{10}	3.97×10^{2}
	0.1	2.18×10^{11}	3.99×10^{3}
	1.0	2.18×10^{12}	3.99×10^{4}
	10.0	2.18×10^{13}	3.99×10^{5}
	100.0	2.18×10^{14}	3.99×10^{6}
4×10^{8}	0.0	2.17×10^{10}	3.97×10^{1}
	0.001	2.17×10^{10}	3.97×10^{1}
	0.01	2.19×10^{11}	4.00×10^{2}
	0.1	2.18×10^{12}	3.99×10^{3}
	1.0	2.18×10^{13}	3.99×10^{4}
	10.0	2.18×10^{14}	3.99×10^{5}
	100.0	2.18×10^{15}	3.99×10^{6}

TABLE 4.2(cont.)

$N = \frac{H^2}{K}$	Re	$(Gr)_c$	$(Ra)_c = \frac{Gr \times Pr}{N}$
$4.\times10^{9}$	0.0	2.15×10^{11}	3.94×10^{1}
	0.001	2.15×10^{11}	3.94×10^{1}
	0.01	2.17×10^{12}	3.97×10^{2}
	0.1	2.18×10^{13}	3.99×10^{3}
	1.0	2.18×10^{14}	3.99×10^{4}
	10.0	2.17×10^{15}	3.99×10^{5}
	100.0	-	-
$4.\times10^{10}$	0.0	2.17×10^{12}	3.97×10^{1}
	0.001	2.17×10^{12}	3.97×10^{1}
	0.01	2.18×10^{13}	3.99×10^{2}
	0.1	2.18×10^{14}	3.99×10^{3}
	1.0	2.18×10^{15}	3.99×10^{4}
$4.\times10^{11}$	0.0	2.15×10^{13}	3.94×10^{1}
	0.01	2.15×10^{13}	3.94×10^{1}
	0.01	2.18×10^{14}	3.99×10^{2}
	0.1	2.18×10^{15}	3.99×10^{3}
	1.0	-	-

TABLE 4.3 SUMMARY OF CRITICAL RAYLEIGH NUMBERS FOR

$0 \leq N \leq 4 \times 10^{-1}$

$Pr = 0.733$

Aspect Ratio = 1 & 2

$\gamma = 1.0$ FOR $N = 0$

$\gamma = 2. \times 10^{-4}$ FOR $N > 0$

N	Re	$(Gr)_c$	$(Ra)_c^*$
0.0	0.0	2.33×10^{3}	1.708×10^{3}
	0.001	2.33×10^{3}	1.708×10^{3}
	0.01	2.33×10^{4}	1.708×10^{4}
	0.1	2.33×10^{5}	1.708×10^{5}
	1.0	2.33×10^{6}	1.708×10^{6}
	10.0	2.33×10^{7}	1.708×10^{7}
	100.0	2.33×10^{8}	1.708×10^{8}
4×10^{-2}	0.0	9.33×10^{1}	1.710×10^{3}
	0.001	9.33×10^{1}	1.710×10^{3}
	0.01	9.31×10^{2}	1.706×10^{4}
	0.1	9.32×10^{3}	1.707×10^{5}
	1.0	9.33×10^{4}	1.710×10^{6}
	10.0	9.33×10^{5}	1.710×10^{7}
	100.0	9.31×10^{6}	1.706×10^{8}

*FOR $N = 0.0$ $(Ra)_c = (Gr \times Pr)$

FIG.4.1 GRASHOF NUMBER VS. REYNOLDS NUMBER AT DIFFERENT VALUES OF NA

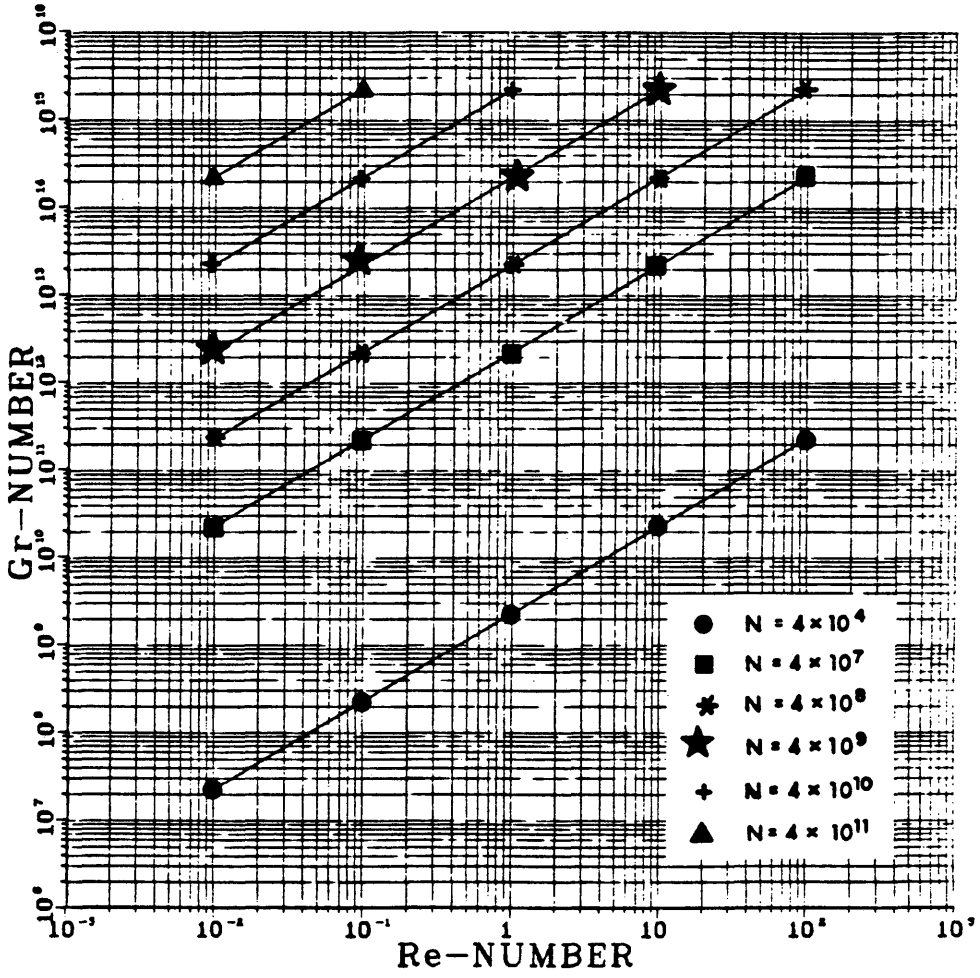

FIG.4.2 GRASHOF NUMBER VS. REYNOLDS NUMBER FOR HIGH PERMEABILITY

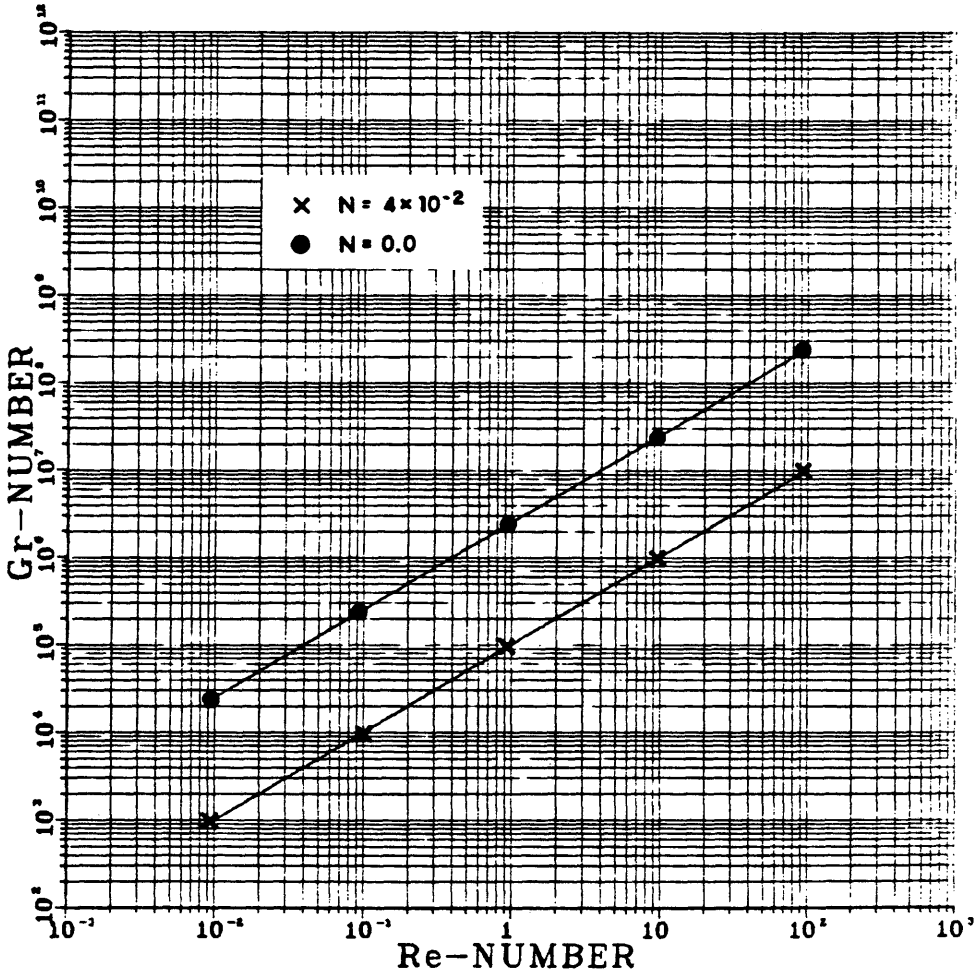

FIG.4.3 CRITICAL RAYLEIGH NUMBERS VS. REYNOLDS NUMBERS

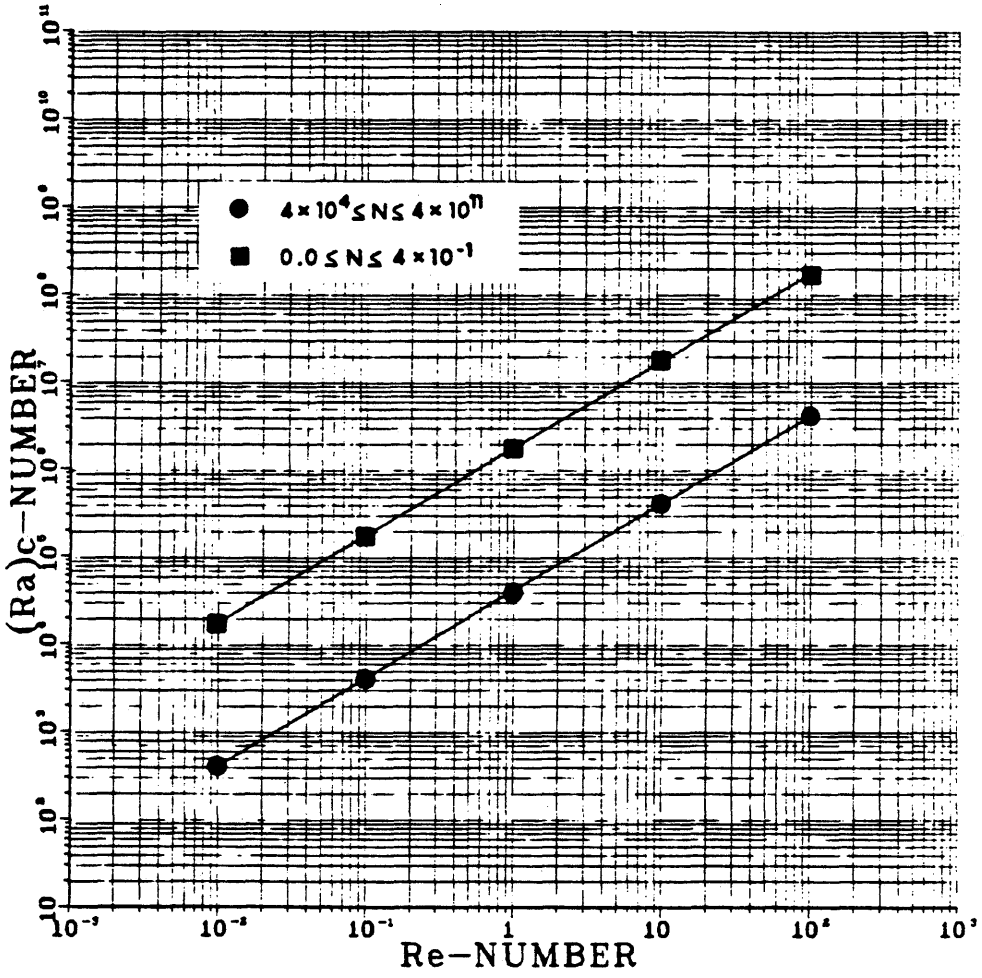

4.3 Streamlines and Isotherms

The numerical solutions to the set of partial differential equations are presented in the form of contour plots of the stream function and the temperature given in Figures (4.4-4.27). The streamlines yield an immediate picture of the flow pattern. The method used here to plot the streamlines and isotherms is described in reference (42). It is simply to print different symbols in the fluid domain, depending on the local values of stream function and temperature.

The examination of iso-therms shows the effect of fluid flow on temperature distribution. The isotherms which are plotted always correspond to,

θ = 0.0, 0.001, 0.003, 0.01, 0.05, 0.2, 0.3, 0.5, 0.6, 0.7, 0.8. 0.9, 1.0.

and the streamlines correspond to

ψ = -2.0, -1.0, -.9, -.8, -.7, -.6, -.5, -.3, -.2, -.05, -.01, -.003, -.001, 0.0, 0.001, 0.003, 0.1, .05, 0.2, 0.3, 0.5, 0.6, 0.7, 0.8, 0.9, 1.0, 2.0.

The symbols correspond to the above values and can be found in Appendix (C-3).

Figures (4.4-4.11) show the streamlines and isotherms for the downflow case and conditions indicated under each

figure at different time steps. It can be seen from the printed symbols that the flow is directed downward. At τ = 0.025 (Figure 4.4) shows a weak convection motion developing the fluid. As time increases convection currents develop in the fluid until finally a steady state is reached. At time τ = 0.5 (Figure 4.7) one vortex is established at the corner where the insulated and the hot bottom intersect. A second vortex forms by the centerline. The vorticies expand towards the sides forming a complete picture of the convect flow pattern at τ = 1.5. The isotherms at τ = 1.5 are shown in Figure (4.12). Figures (4.13 and and 4.14) are the streamlines and the isotherms for the downflow case of a highly permeable medium. It shows the anti-clock-wise vortex which expands towards the sides and the bulk of the fluid as time increases until τ = 1.5 where it is considered the steady state.

The streamlines and isotherms for the upflow case in porous media are shown in Figures (4.17-4.18). At τ = 0.0075 a small convection cell starts at the lower left corner. As time increases a second cell forms by the centerline and the flow pattern expands towards the sides.

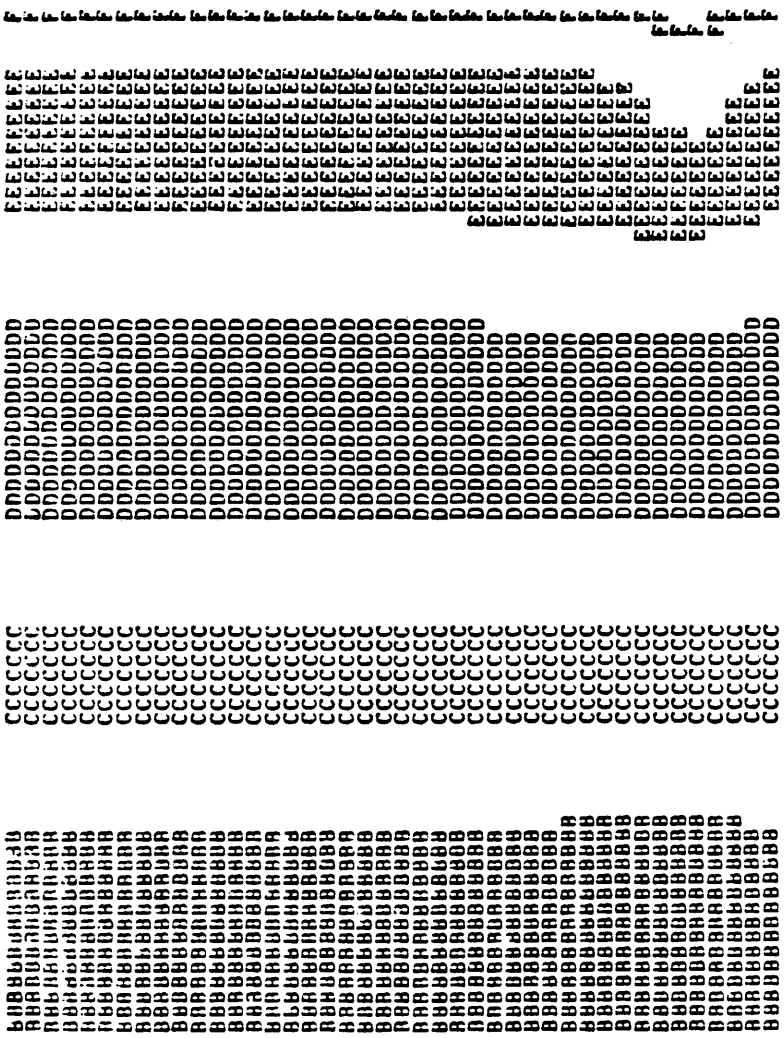

FIGURE 4.4 STREAMLINES FOR POROUS MEDIA (DOWNFLOW) τ = 0.025

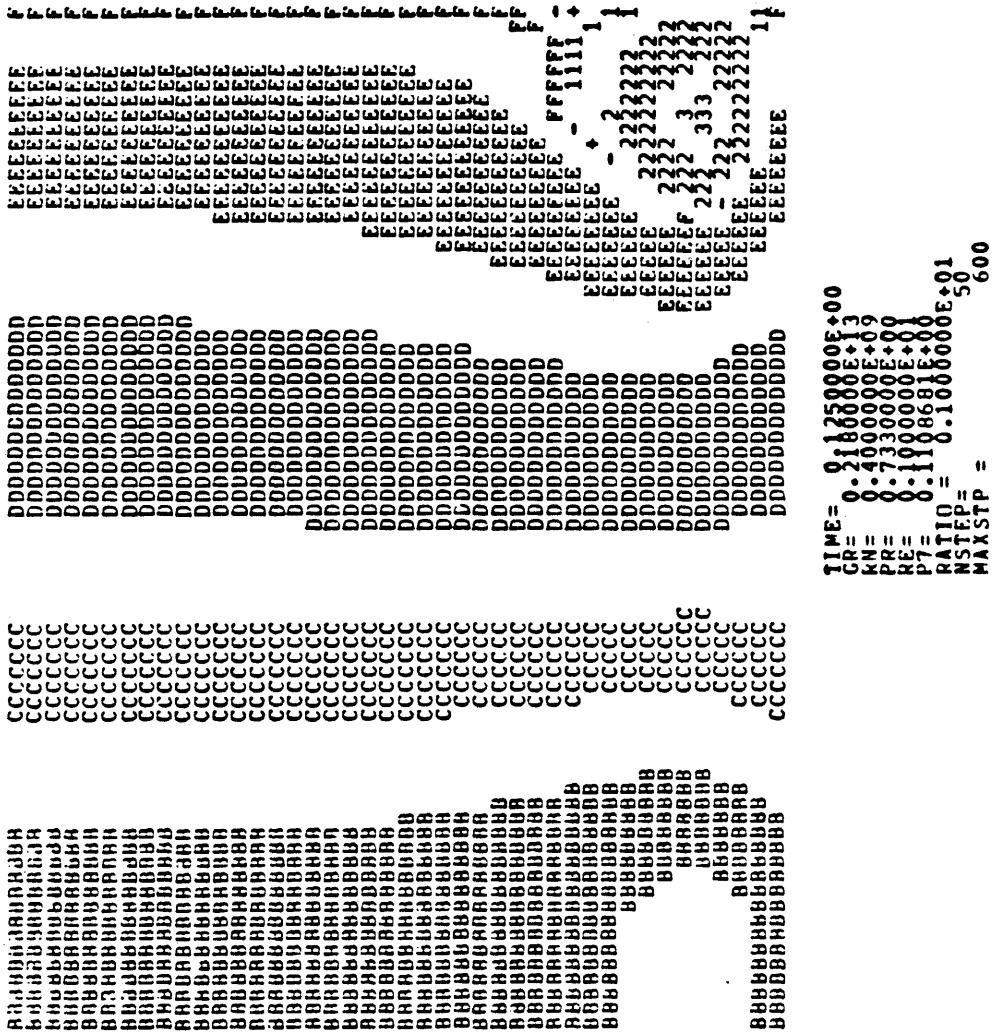

FIGURE 4.5 STREAMLINES FOR POROUS MEDIA (DOWNFLOW) τ = 0.125

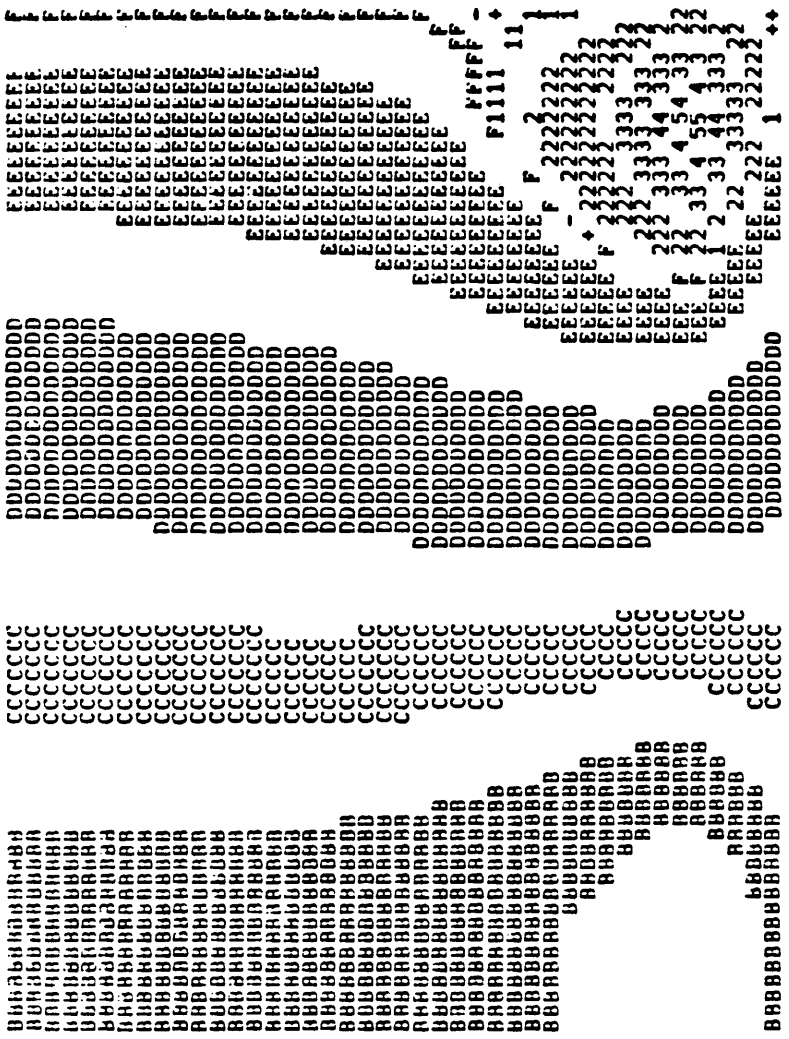

FIGURE 4.6 STREAMLINES FOR POROUS MEDIA (DOWNFLOW) τ = 0.25

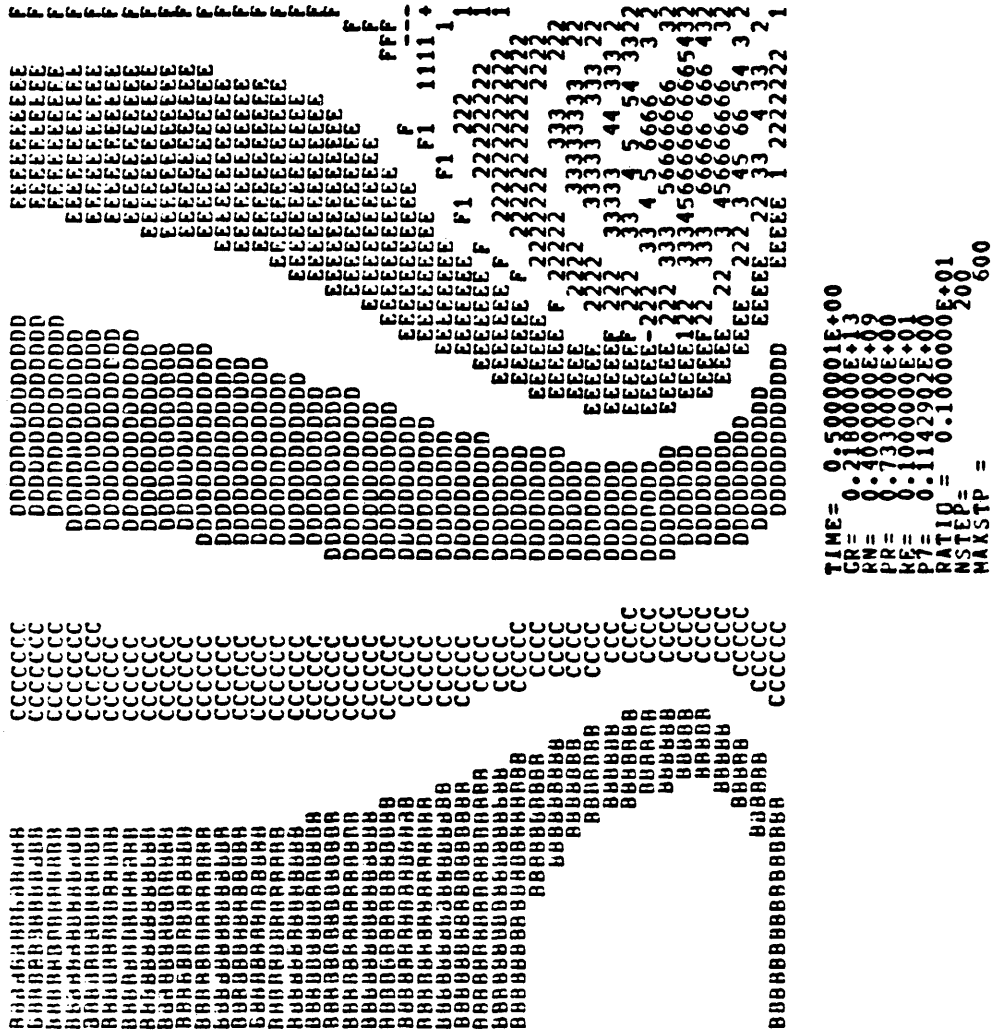

FIGURE 4.7 STREAMLINES FOR POROUS MEDIA (DOWNFLOW) τ = 0.5

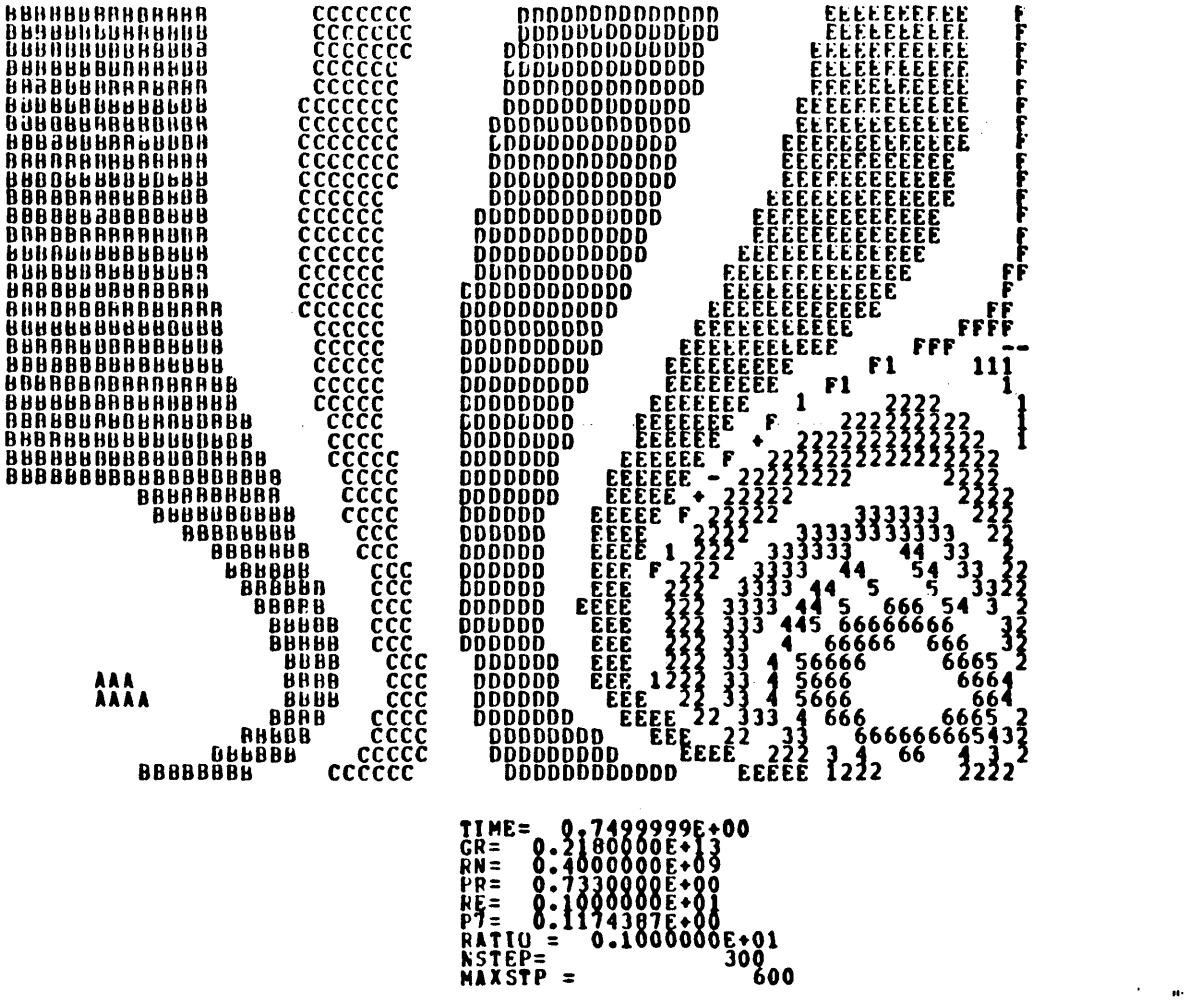

FIGURE 4.8 STREAMLINES FOR POROUS MEDIA (DOWNFLOW) τ = 0.75

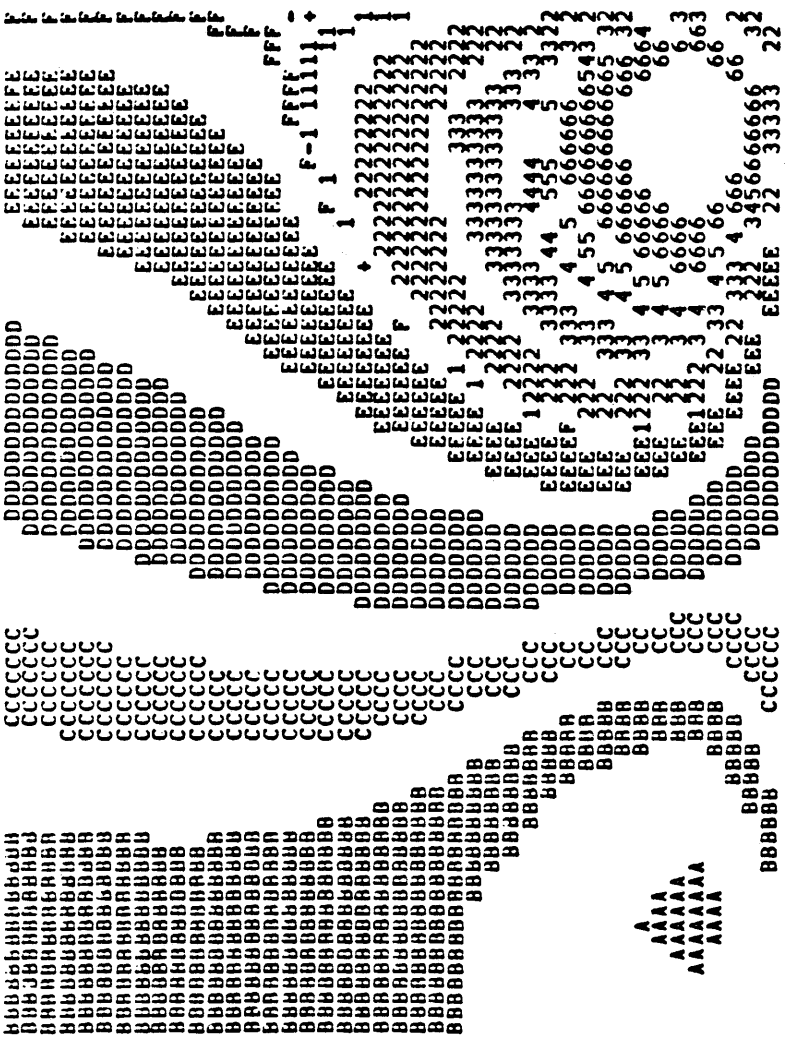

FIGURE 4.9 STREAMLINES FOR POROUS MEDIA (DOWNFLOW) τ = 1.0

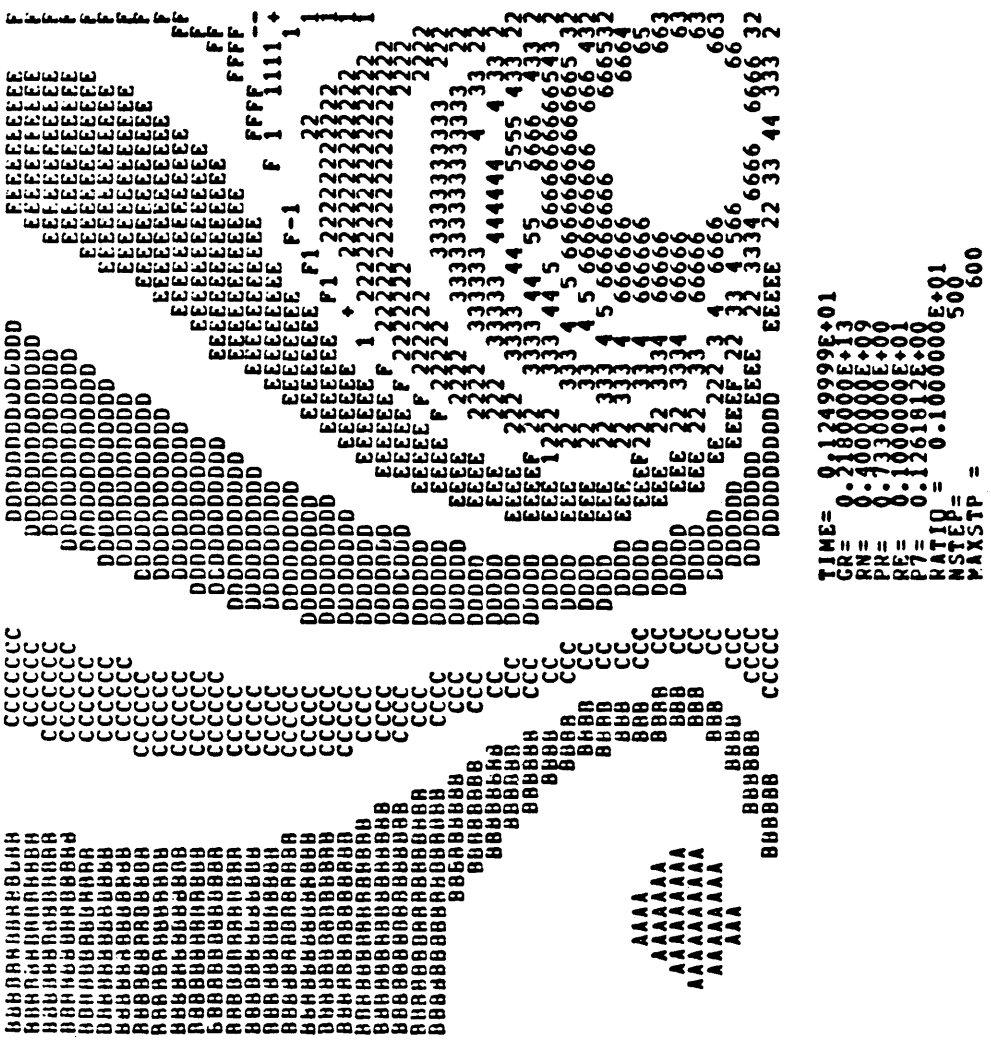

FIGURE 4.10 STREAMLINES FOR POROUS MEDIA (DOWNFLOW) τ = 1.25

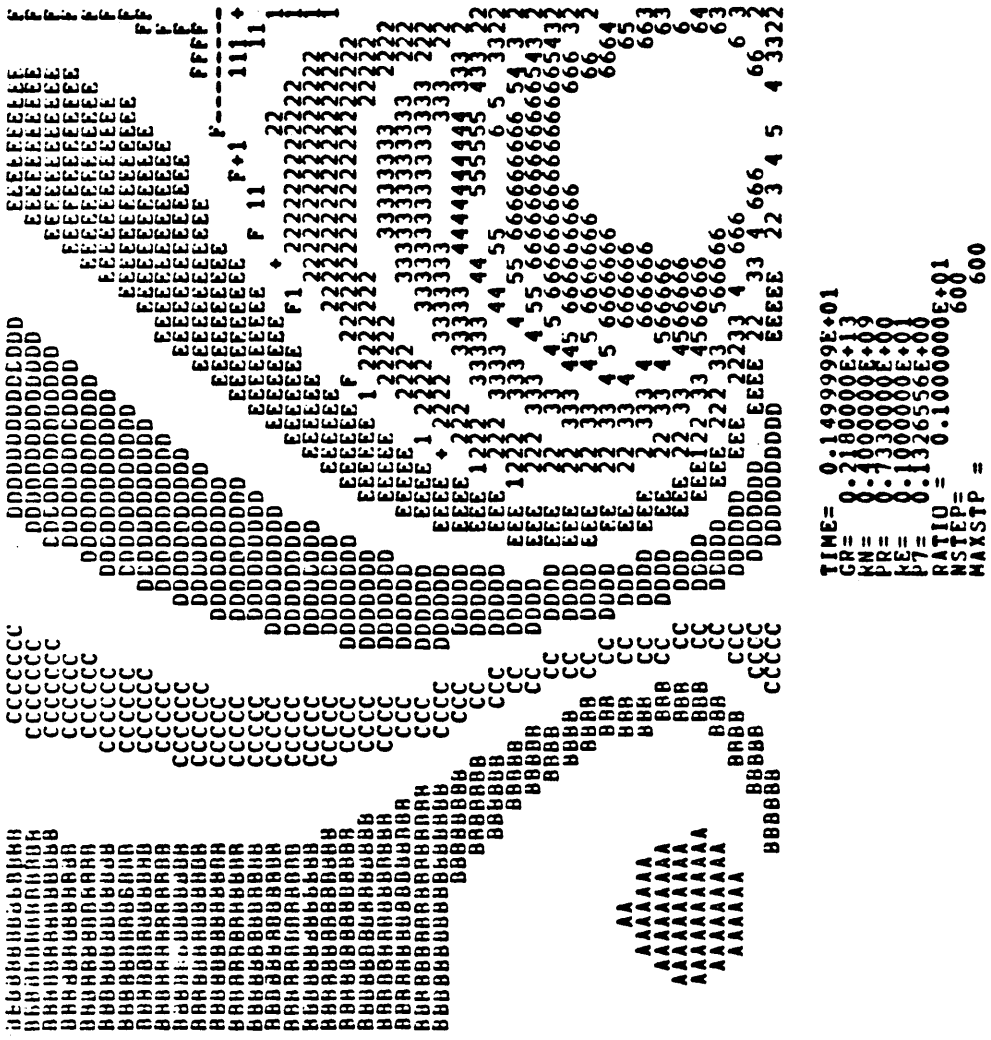

FIGURE 4.11 STREAMLINES FOR POROUS MEDIA (DOWNFLOW) τ = 1.5

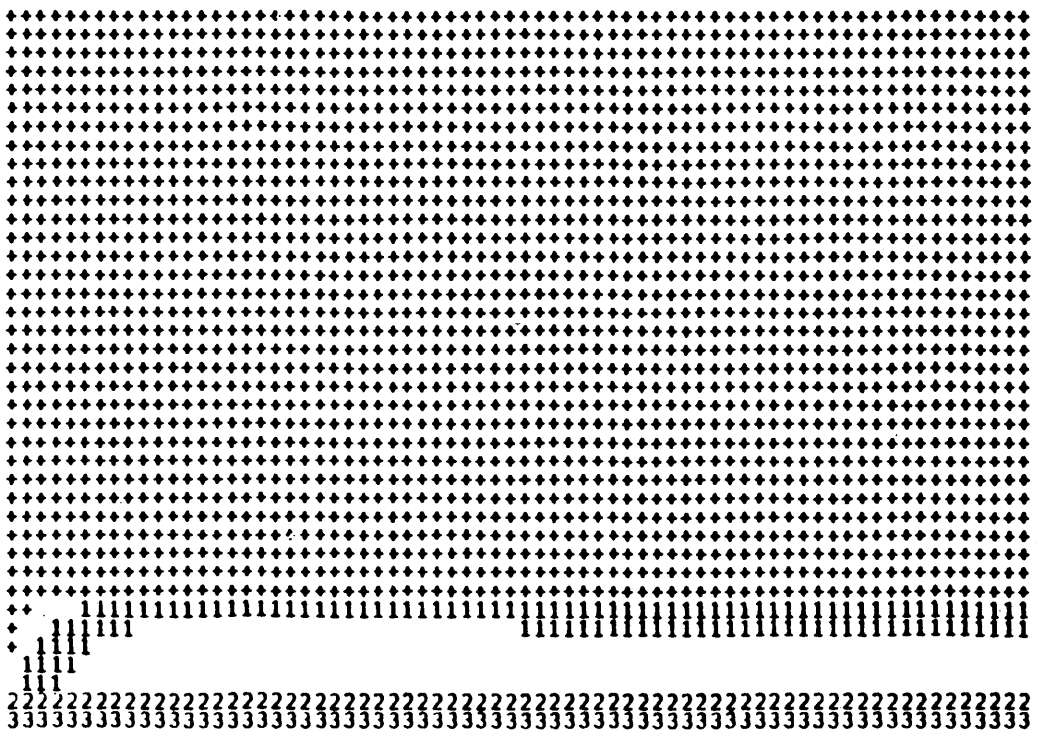

FIGURE 4.12 ISOTHERMS FOR POROUS MEDIA (DOWNFLOW) $\tau = 1.5$

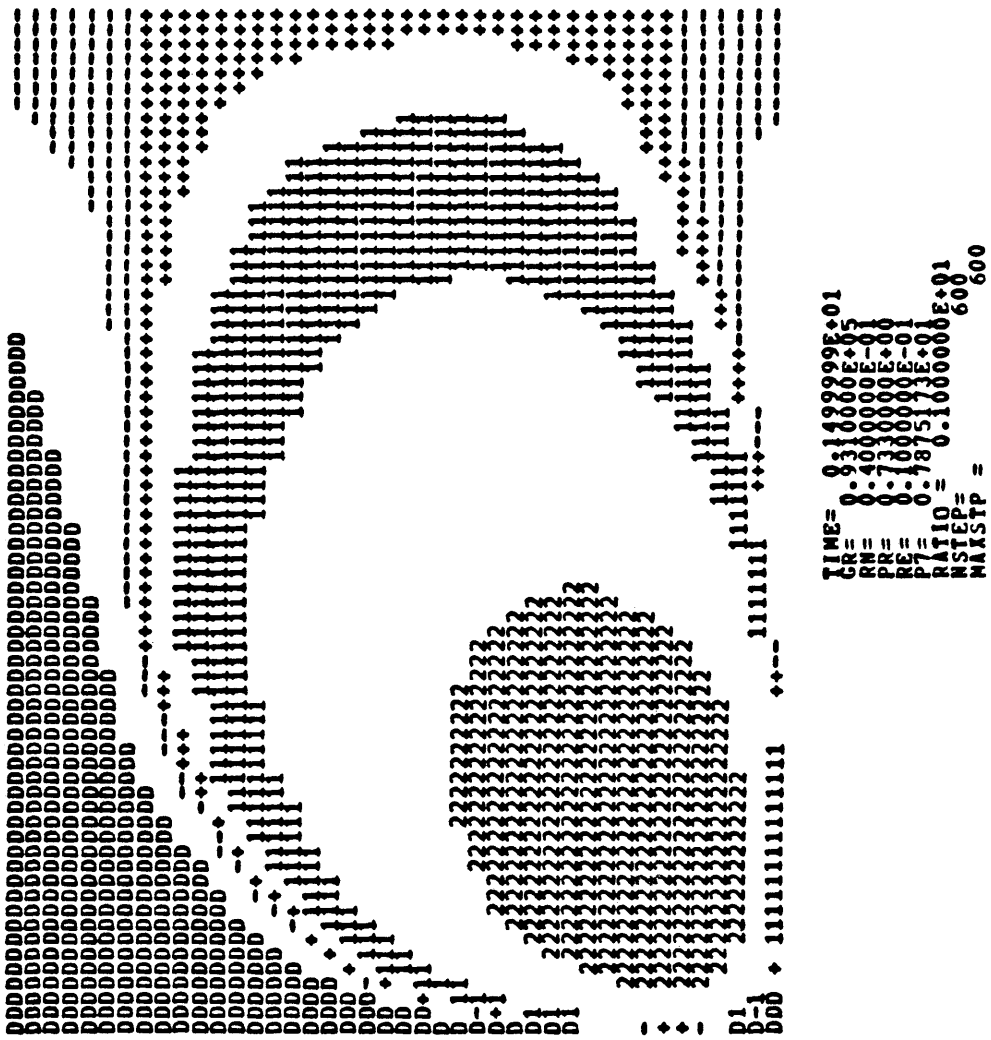

FIGURE 4.13 STREAMLINES FOR HIGHLY PERMEABLE MEDIA (DOWNFLOW), τ = 1.5

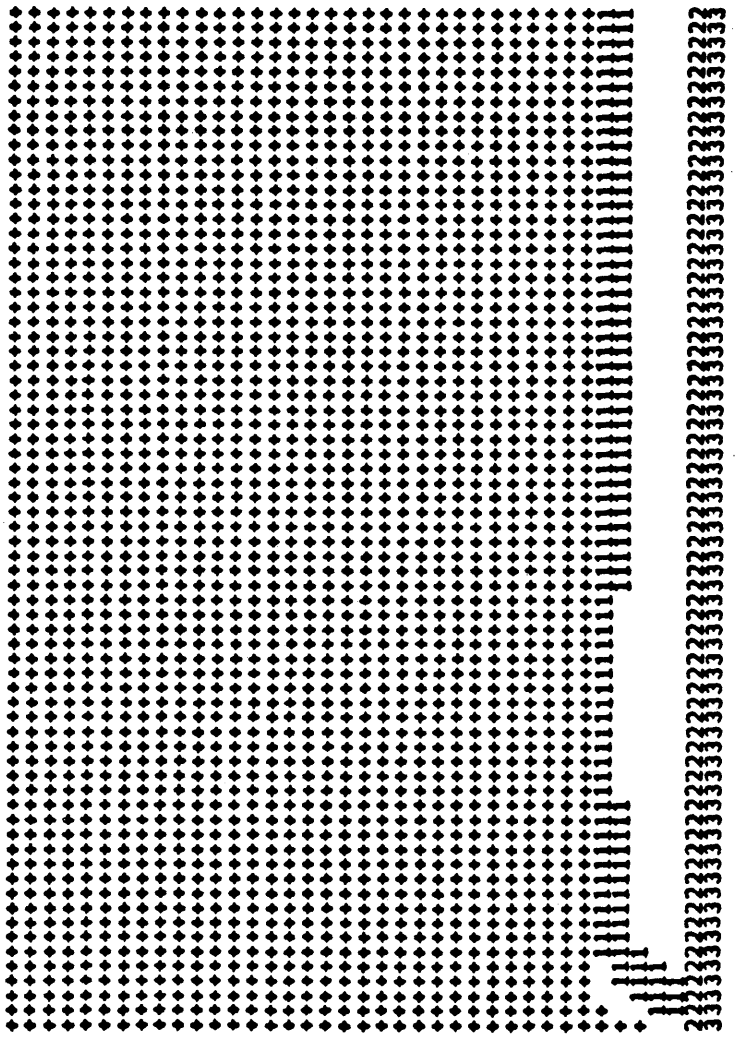

FIGURE 4.14 ISOTHERMS FOR HIGHLY POROUS MEDIA (DOWNFLOW) τ = 1.5

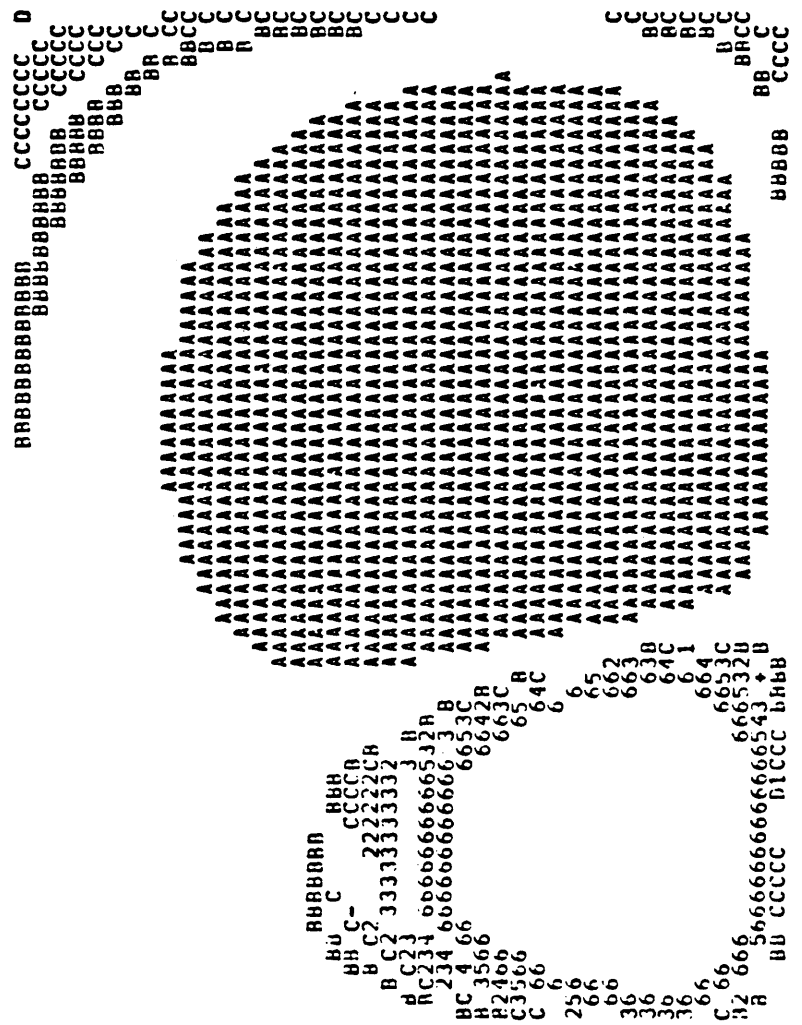

FIGURE 4.15 STREAMLINES FOR SINGLE PHASE FLUID (DOWNFLOW) $\tau = 1.5$

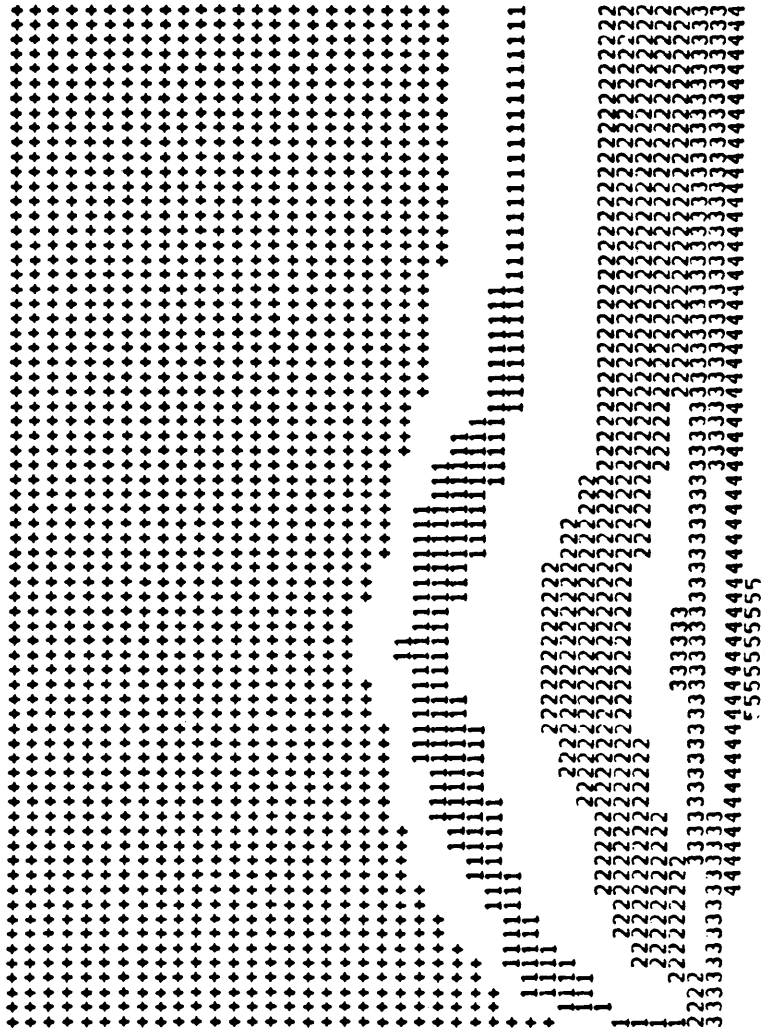

FIGURE 4.16 ISOTHERMS FOR SINGLE PHASE FLUID (DOWNFLOW) $\tau = 1.5$

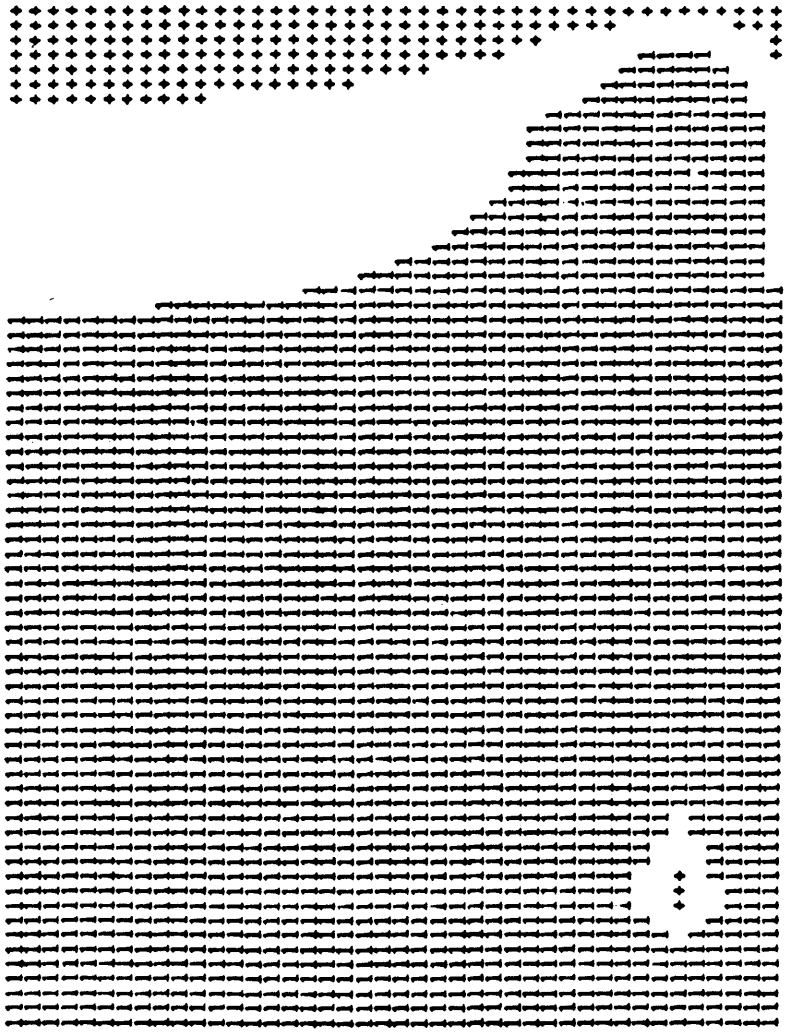

FIGURE 4.17 STREAMLINES FOR POROUS MEDIA (UPFLOW), τ = 0.0075

FIGURE 4.18 STREAMLINES FOR POROUS MEDIA (UPFLOW) τ = 1.5

Attention will now be directed to an examination of the streamlines and iso-therms of Figures (4.19-4.24), which represent the final stages in the solution of the non-flow case. At τ = 1.5 (Figure 4.19) the fluid flow pattern consists of two vortices, the one in the left is in the anti-clock-wise direction and the other in the right is in the clock-wise direction. Little further change occurs to these vorticies when time increased beyond τ = 1.5. Figure (4.20) shows the iso-therms have moved into the fluid and it can be seen that they are slightly distorted due to the fluid motion. Figures (4.21 - 4.22) represent the flow patterns and the iso-therms for the non-flow case of single-phase fluid at time τ = 1.5. Following these are Figures (4.23 - 4.24), which show the convection currents of the non-flow case of highly permeable media.

It must be noted here that all the above mentioned figures correspond to an aspect ratio of one, and all of which correspond to values computed for a 10 x 10 grid.

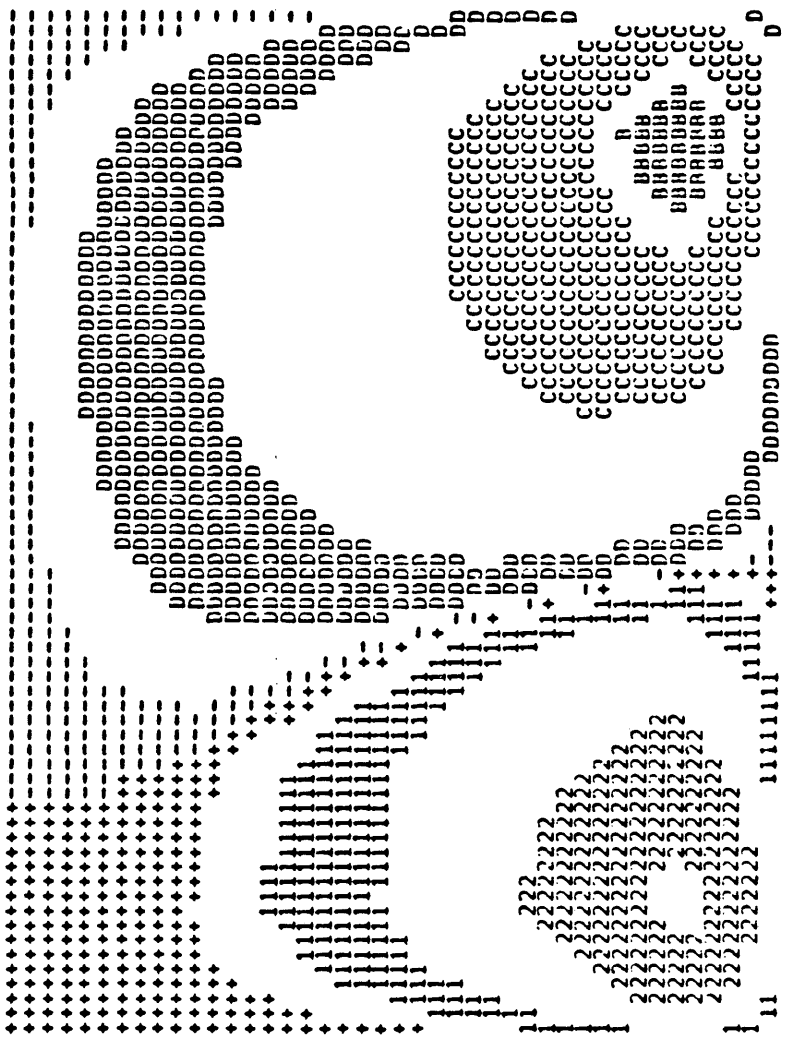

FIGURE 4.19 STREAMLINES FOR POROUS MEDIA (NON-FLOW CASE)

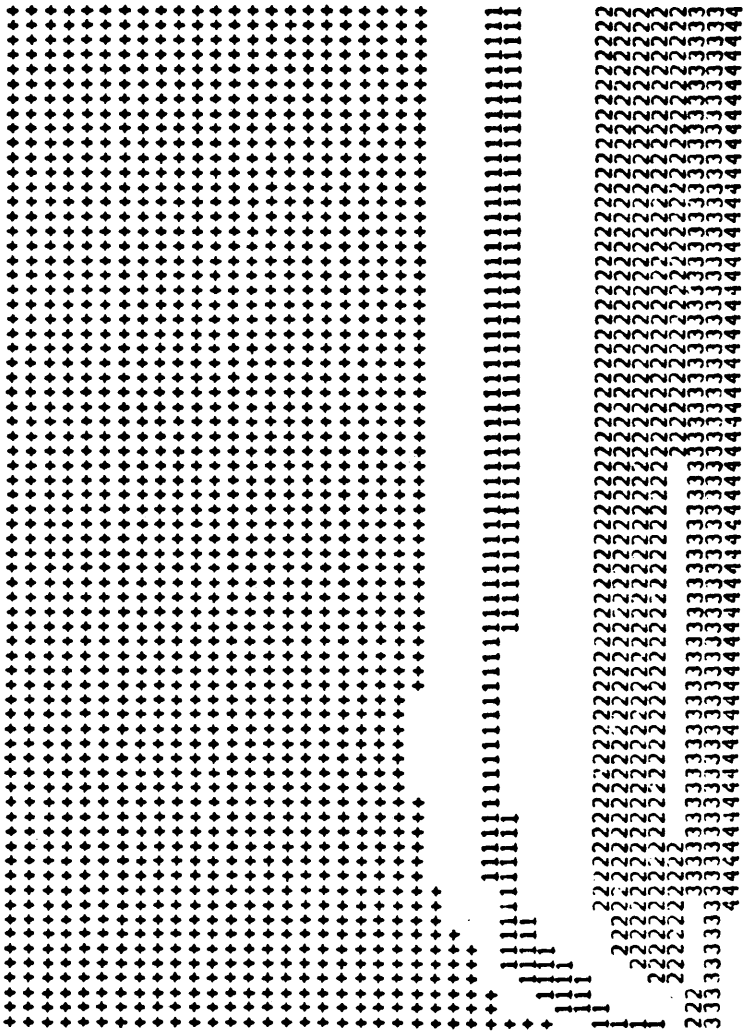

FIGURE 4.20 ISOTHERMALS FOR POROUS MEDIA (NON-FLOW CASE)

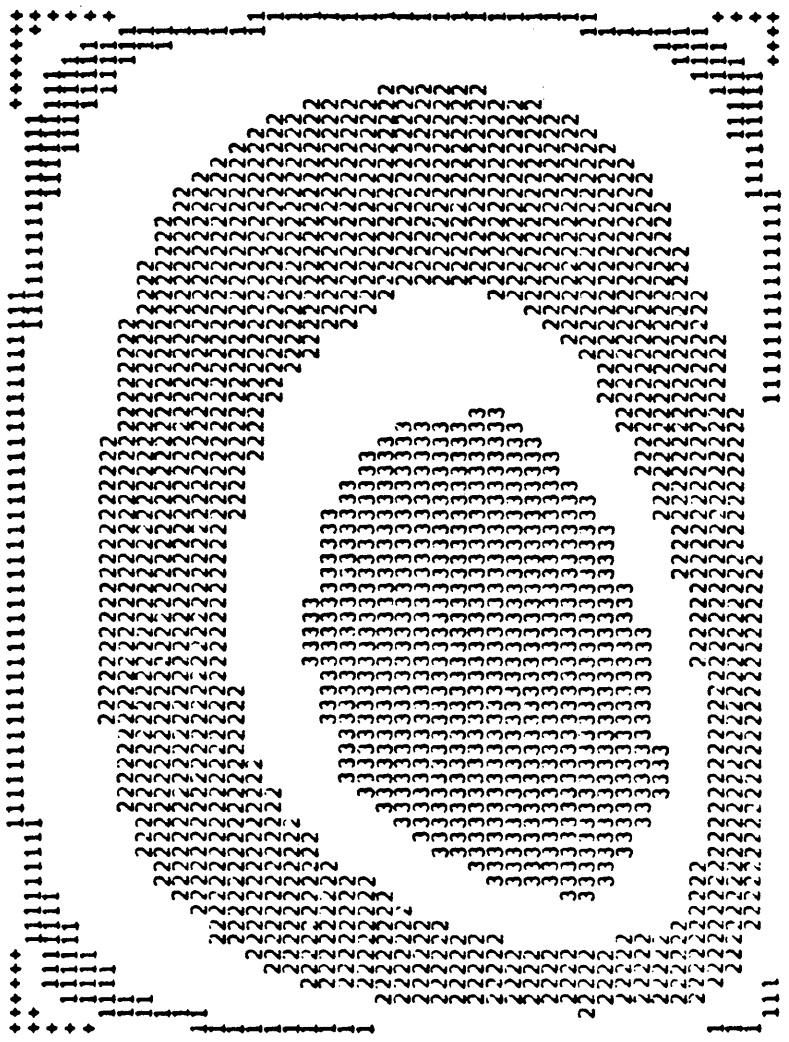

FIGURE 4.21 STREAMLINES FOR SINGLE PHASE FLUID (NON-FLOW) τ = 1.5

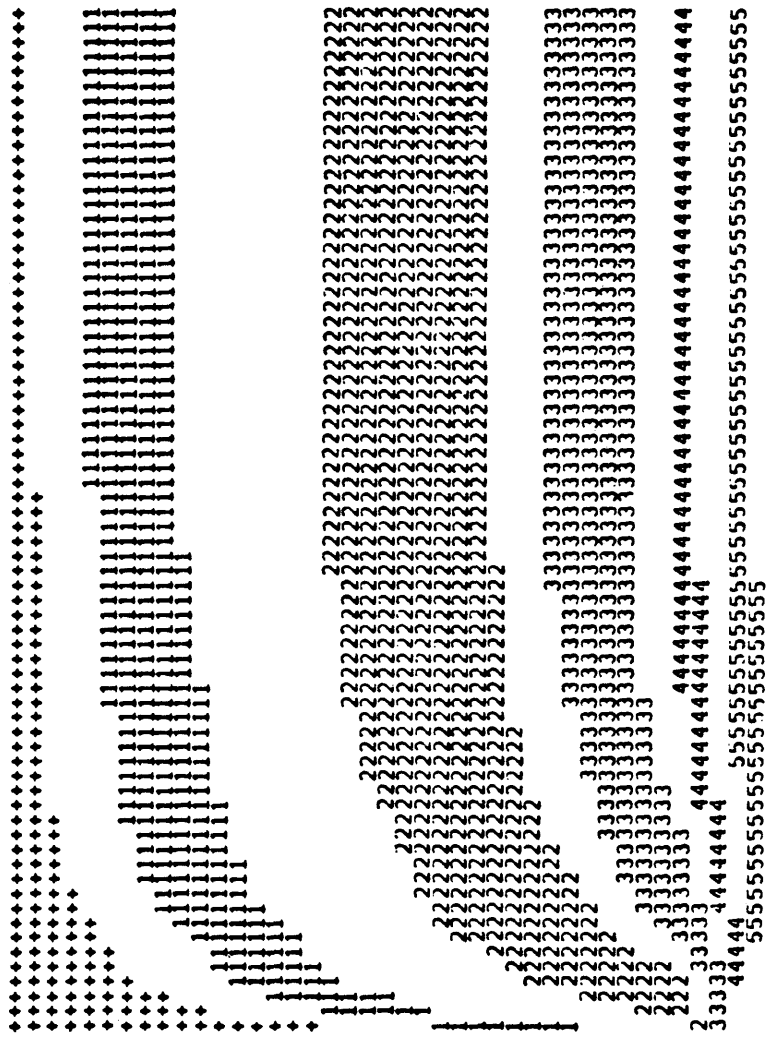

FIGURE 4.22 ISOTHERMS FOR SINGLE PHASE FLUID (NON-FLOW), τ = 1.5

FIGURE 4.23 STREAMLINES FOR HIGHLY PERMEABLE MEDIA (NON-FLOW) $\tau = 1.5$

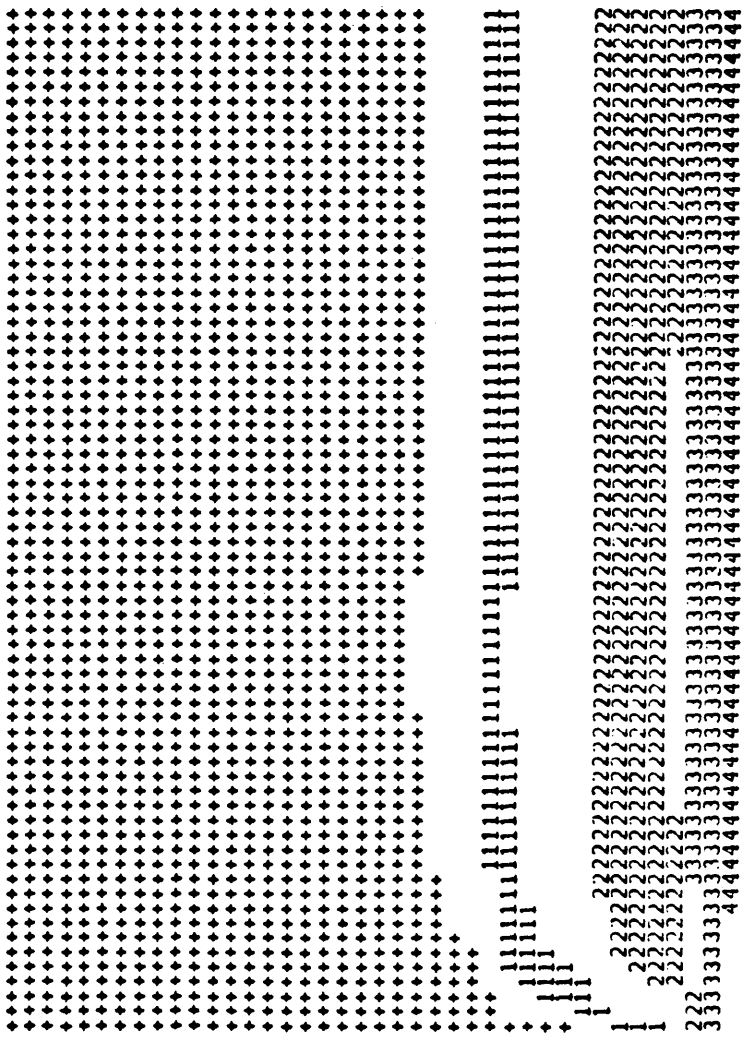

FIGURE 4.24 ISOTHERMS FOR HIGHLY PERMEABLE MEDIA (NON-FLOW) τ = 1.5

Figures (4.25-4.27) show the streamlines for different aspect ratio. Figure (4.25) shows the streamlines for the downflow case with aspect ratio - 0.5 at time τ = 1.5. Comparison with Figure (4.11) where the aspect ratio was 1.0 shows no fundamental change in the flow pattern. Figure (4.26) shows the streamlines for the upflow case with an aspect ratio of two and τ = 1.5. This can be compared to Figure (4.18). Figure (4.27) presented the case for non-flow with an aspect ratio = 2.0 which can be similarly compared to Figure (4.19). Figures (4.26 - 4.27) correspond to values computed for 21 x 9 grid.

It is concluded that within the range of aspect ratios considered, the flow structure is unaffected.

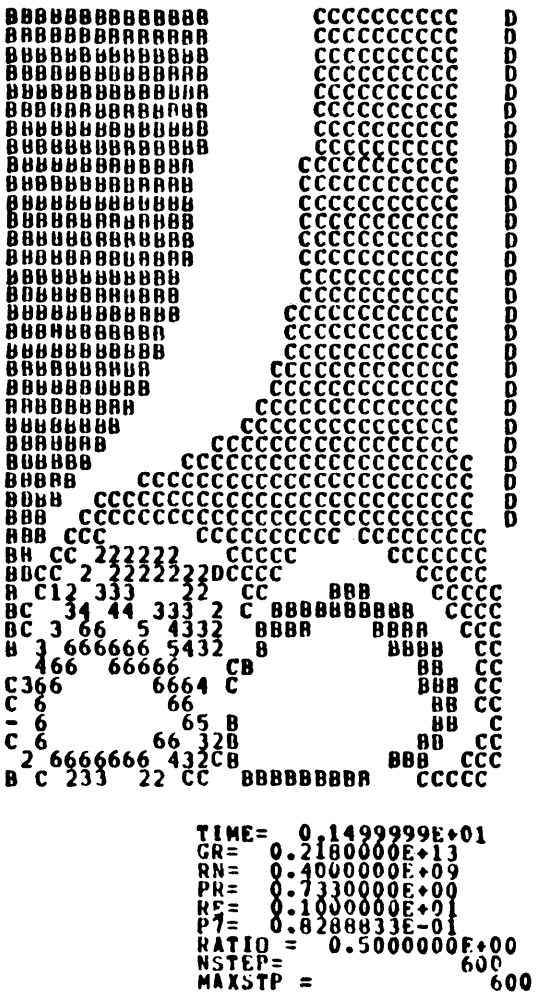

FIGURE 4.25 STREAMLINES FOR POROUS MEDIA (DOWNFLOW) ASPECT RATIO = 0.5

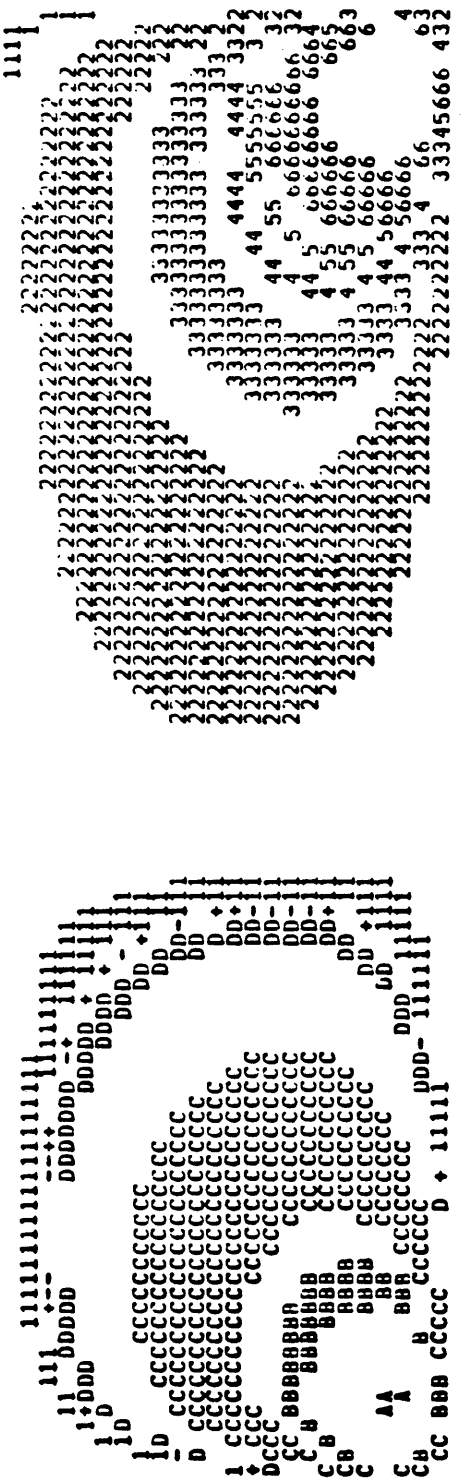

FIGURE 4.26 STREAMLINES FOR POROUS MEDIA (UPFLOW), ASPECT RATIO = 2.0

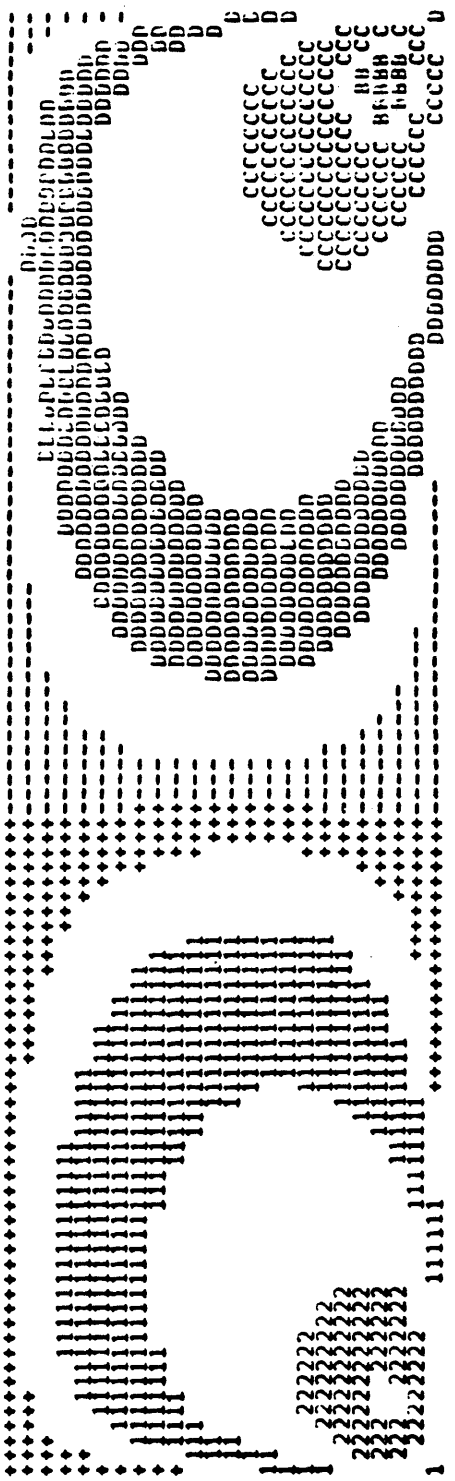

FIGURE 4.27 STREAMLINES FOR POROUS MEDIA(NONFLOW) ASPECT RATIO = 2.0

4.4 Application to Oil Shale Retort

Typical permeabilities for oil shale retorts were calculated from experimental pressure drop data given by Raley (47).

Then Darcy-Rayleigh numbers and Reynolds numbers were established from typical retort operating conditions. These were calculated in terms of a variable height H, above the combustion zone and for a fixed gas velocity of 3 ft/hr. The latter value is considered to be a rather low value for retort operation. An operating line can then be plotted on a graph of Darcy-Rayleigh number vs. Reynolds number with H as the variable. This has been done in Figure (4.28) for values of permeability ranging between 3.0×10^{-8} and 4.0×10^{-4} ft ^{2} and for values of km, of 0.0414 and 0.0265 Btu/hr. ft ^{o}F. These values of km are actually the conductivities of air at 1500 ^{o}F and 600^{o}F respectively, and represent lower bounds to the possible values of bed conductivity. The ranges of these two quantities represent an estimate of the uncertainty in the prediction of typical retort parameters.

Also on Figure (4.28) is shown the critical Darcy-Rayleigh number line of Figure (4.3). It is clear that under normal operating conditions, typical retorts will not be affected by convective flow instability. The only

TABLE 4.4 SUMMARY OF VALUES OF Ra AND Re AT DIFFERENT VALUES OF H

k_m (Btu/hr-ft^{o}F)	K (ft^2)	H(m)	RaK/H^2	Re
0.0414	1.36×10^{-6}	1	1.3×10^{2}	1.88
		2	2.6×10^{2}	3.76
		10	1.3×10^{3}	18.8
		20	2.6×10^{3}	37.6
		50	6.5×10^{3}	94.0
	8.37×10^{-6}	1	9.57×10^{2}	2.23
		2	1.914×10^{3}	4.47
		10	9.57×10^{3}	22.3
		20	1.914×10^{4}	44.6
		50	4.785×10^{4}	111.7
0.0265	$4.\times10^{-4}$	1	5.9×10^{4}	5.05
		10	5.9×10^{5}	50.5
		20	1.18×10^{6}	101.0
		50	2.95×10^{6}	252.6
	$3.\times10^{-8}$	1	4.4	5.05
		10	44.0	50.5
		20	88.0	101.0
		50	2.2×10^{2}	252.5

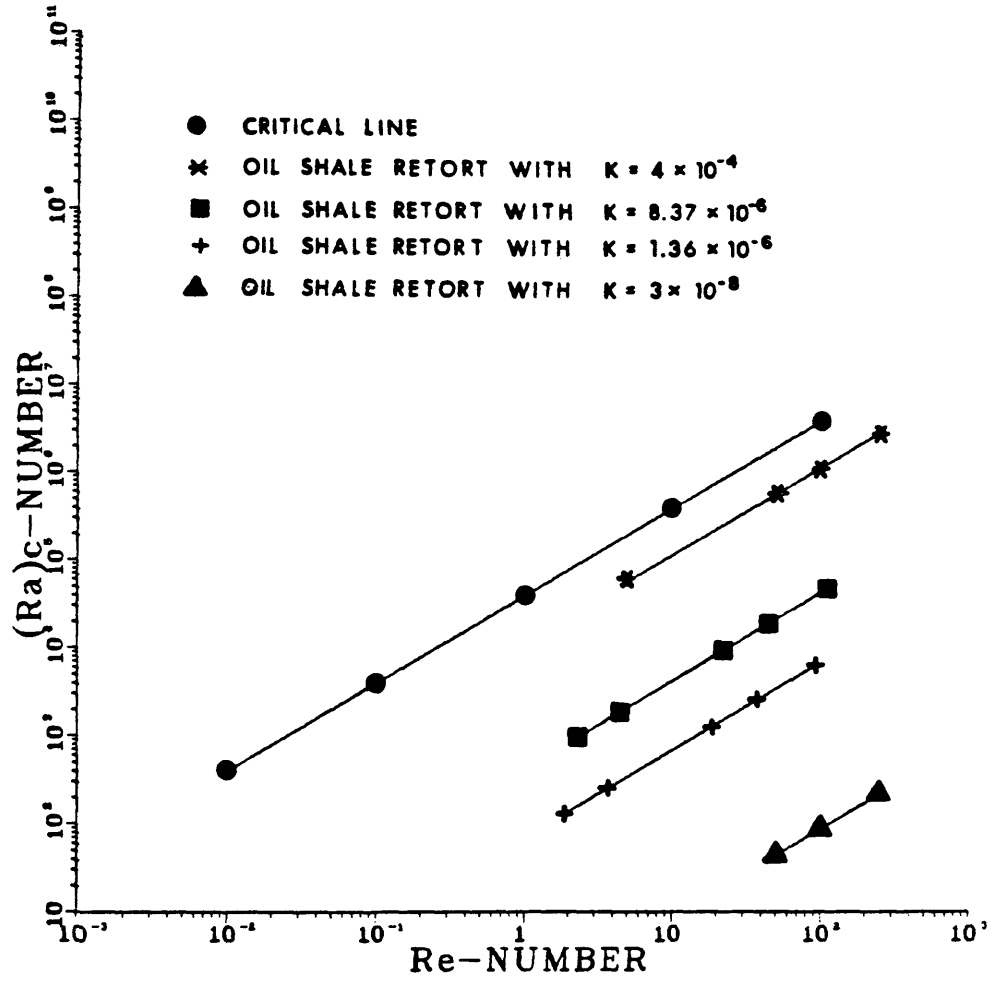

FIGURE 4.28 STABILITY ESTIMATE FOR TYPICAL OIL SHALE RETORT

case where this might occur would be if the gas flow were temporarily stopped and the Rayleigh number were to be zero. This would be represented on the figure by a horizontal line drawn from any of the operating lines to intersect the Darcy-Rayleigh number axis. As is seen, all would intersect above the non-flow critical value of $4\pi^2$.

The following is an example of the calculations.

1. Calculation of Permeability

From Darcy's Law neglecting the gravity effect,

$K = \mu V/\Delta P$

μ, V, ΔP are taken from Appendices A-1,A-2 at 1500^oF

$$K = \frac{0.038 \times 0.10575}{3600 \times 0.816}$$

$$k = 1.36 \times 10^{-6} \text{ ft}^2$$

2. Calculation of Rayleigh number:

$$Ra = \frac{g\beta\Delta T \, H^3(\rho Cp)_f}{\nu \, k_m} \cdot \frac{K}{H^2}$$

$\beta = 1/T_o$, $T_o = 70^oF$

ρ,Cp, V, k_m are taken from Appendix B-1.

$$Ra = \frac{32.2 \times 1.88 \times 10^{-3} \times 1430 \times 3600 \times 3600 \times 5.6 \times 10^{-3} \times 1.36 \times 10^{-6}}{5.225 \times 0.0414} H$$

$Ra = 39.65\ H$, H is the depth of combustion zone.

3. Reynolds number

for fluid velocity of 3 ft/hr = 8.33×10^{-4} ft/sec.

$$Re = \rho v_o H/\mu$$

$$= \frac{0.02024 \times 8.33 \times 10^{-4}}{(0.10575/3600)} H$$

$$Re = 0.575\ H$$

When (K) the permeability and k_m the conductivity are changed, different values of Re and Ra will be found by the same method as above. Rayleigh numbers and Reynolds numbers can be calculated as a function of (H). Table 4.4 shows a summary of those numbers at different values of (H).

4.5 Stability of the Numerical Method

According to the quasilinear analysis of Lox and Richtmyer (48) applied to the energy equaiton and to vorticity equation in dimensionless form, the numerical method is stable if the following stability criterion is satisfied.

1. For energy equation and when N = 0 in the vorticity equation

$$\Delta\tau \leq \left(\frac{1}{2h}(Uf+|Uf|-Ub+|Ub|+Vf+|Vf|-Vb+|Vb|) + 4/h^2 Pr\right)^{-1}$$

2. For the vorticity equation expressed in terms of Brinkmann's extension of Darcy's Law

$$\Delta\tau \leq \left(\frac{1 - N}{1/2h(Uf+|Uf|-Ub+|Ub|+Vf+|Vf|-Vb+|Vb|)+4/h^2Pr}\right)$$

where $N = \frac{H^2}{K}$

The right hand side of the second equation is defined as (P7) in the computer program, the right hand side of the first equation is also defined as (P7) with N = 0. The values of (P7) are calculated at various time steps and shown under every figure of Figures (4.4 - 4.27) and summarized in Table (4.5).

It is seen that P7 usually decreases as the calculation proceeds in time, but nowhere was a value less than $\Delta\tau$ encountered. This supports the conclusion that the computations were stable.

4.6. Validity of the Results

Three types of checks were made from which the results were considered valid:

1. The comparison with the published theoretical work was mentioned in Section (4.1) for the porous medium non-flow case, and with the Benard convection problem for single phase fluid. The comparison was in excellent agreement.

TABLE 4.5 SUMMARY OF THE CRITERION OF THE NUMERICAL STABILITY OF THE ENERGY AND VORTICITY EQUATIONS ($\Delta\tau$ = 0.0025)

Vorticity Eqn. Expressed in Terms of	Re	Vorticity		Energy	
		Time	P7	Time	P7
1. Navier Stokes Equation	0.0	0.025	0.14	0.025	0.14
		1.5	0.12	1.5	0.12
	1.0	0.025	0.092	0.025	0.092
		1.5	0.017	1.5	0.017
2. Brinkman's Extension of Darcy's Law	0.0	0.025	14.2	0.025	1.42
		1.5	7.7	1.5	0.69
	0.1	0.025	5.9	0.025	5.9
		1.5	7.8	1.5	7.8
3. Darcy's Law	0.0	0.025	-	0.025	1,42
		1.5	-	1.5	0.13
	1.0	0.025	-	0.025	0.123
		1.5	-	1.5	0.12

2. The numerical stability of the method was checked. Calculations of the criteria P7 (see Table (4.5)) support the conclusion that the computations were stable, Section (4.5).

3. Different grid systems were used and it was found that they gave almost the same results for critical Darcy-Rayleigh numbers as shown in Table (4.6).

TABLE 4.6 COMPARISON OF RESULTS AT DIFFERENT GRID

N	Re	Grid	(Gr)c	Ra K/H^2
4×10^9	0.0	10x10	2.15×10^{11}	3.94×10^1
		20x20	2.15×10^{11}	3.94×10^1
	1.0	10x10	2.18×10^{14}	3.99×10^4
		20x20	2.17×10^{14}	3.97×10^4

CHAPTER V

CONCLUSIONS

From the results obtained the following may be concluded:

1. For the non-flow case, the critical Darcy-Rayleigh number is found to be $Ra\frac{K}{H^2} = 39.6$ in agreement with published theoretical values. This is verified for the permeability range $4x10^4 \leq N \leq 4x10^{11}$. In the high permeability limit ($4x10^{-2} \leq N \leq 4x10^{-1}$) a critical Darcy-Rayleigh number of 1710 is found. For the single phase fluid, a critical Rayleigh number of 1710 is also found in agreement with the well-known result for Bénard convection. Wall effects do not appear to be important.

2. For the flow case, a linear relationship between critical Rayleigh number and Reynolds number is found for Reynolds numbers ranging from 10^{-3} to 10^2. The critical Rayleigh number is constant for the non-flow case.

3. Neither aspect ratio nor the flow direction (upflow vs downflow) affect the values of the critical Darcy-Rayleigh number.

4. The numerical method is considered to be computationally stable in the range of interest.

5. For application to oil shale retorts, it is concluded that a typical oil shale retort is convectively stable under normal operating conditions.

CHAPTER VI

RECOMMENDATIONS

From the results and conclusions it is recommended to:

1. Visualize the convection motion of fluid flow through porous media and measure the temperature distribution experimentally, if possible.

2. Extend the present work for other coordinates (for example, cylindrical coordinates).

3. Modify the method used to solve the non-linear partial differential equations for the problem of Reynolds numbers higher than 100, where this method fails to converge.

4. Modify the boundary conditions when other coordinates are used.

5. Study the nature and the effect of internal heat generation.

NOMENCLATURE

Roman Letter	Definition
Cp	Specific heat
Gr	Grashof number = $g\beta\Delta TH^3/\nu^2$
g	Acceleration due to gravity
H	Height of the porous bed
h	Grid spacing in x or y direction
K	Permeability of the fluid
km	Thermal conductivity of the (fluid medium satruated porous layer)
L	Width of the bed
M	Number of grid spacing in the x-direction
N	Number of grid spacing in the y-direction
N	Reciprocal of dimensionless permeability = $\frac{H^2}{K}$
P	Pressure
PR	Reference pressure
Pr	Prandtl number, = $\mu Cp/km$
Ra	Rayleigh number, = $g\beta\Delta TH/\nu\alpha_m$
t	Time
T	Temperautre
ΔT	Temperature difference, = (T_2-T_1)
u	Velocity in the x-direction
U	Dimensionless velocity in x-direction

Roman Letter	Definition
v	Velocity in the y-direction
V	Dimensionless velocity in y-direction
w	Dimensionless vorticity
x	Horizontal coordinate, measured from the bottom left hand corner
X	Dimensionless horizonal coordinate
y	Vertical coordinate measured upwards from the bottom left hand corner
Y	Dimensionless vertical coordinate

Greek Letter	Definition
α	Thermal diffusivity
α_m	Thermal diffusivity of the medium
β	Volume coefficient of thermal expansion = 1/To
γ	Heat capacity ratio, $(\rho C_p)_f/(\rho C_p)_m$
ΔX	Grid spacing in x-direction
ΔY	Grid spacing in y-direction
θ	Dimensionless temperature, $= \frac{T-T_0}{T_1-T_0}$
$\Delta\tau$	Dimensionless time increment
τ	Dimensionless time
∇^2	Laplacian operator, $= \frac{\partial^2}{\partial X^2} + \frac{\partial^2}{\partial Y^2}$

Greek Letter	Definition
ξ	Vorticity
μ	Viscosity
ν	Kinematic viscosity
ρ	Density
ψ	Dimensionless stream function
ω	Relaxation parameter
ω_{opt}	Optimum relaxation parameter

Subscripts

0	Refers to conditions at time t = 0
1	Refers to the hot side
f	Refers to fluid, or forward
i	Denotes a grid point whose horizontal coordinate is x = i x
j	Denotes a grid point whose vertical coordinate is Y = jΔY
R	Denotes reference quantity
m	Refers to medium
n	Refers to number of time steps
γ	Refers to ratio $(\rho Cp)_f/(\rho Cp)_m$

LITERATURE CITED

1. Benard, H., "Lee Tourbillons Cellulaires Dans Une Nappe Liquide, Methods Optiques D'obersavation et D'Enregistrement," J. dePhysique, 10, 254, (1901).

2. Rayleigh, Lord, "On Convective Currents in a Horizontal Layer of Fluid when the Higher Temperature is on the Under Side," Phil. Mag., 32, 529-546 (1916).

3. Pellew, A. and Southwell, R. V., "On Maintained Convective Motion in a Fluid Layer Heated from Below," Proc. Roy. Soc. London, A, 176, 312-343 (1940).

4. Malkus, W. V. R. and Veronis, G., "Finite Amplitude Cellular Convection," J. Fluid Mech., 4, 225-260, (1958).

5. Schluter, A. D., Lortz and Busse, F., "On the Stability of Steady Finite Amplitude Cellular Convection," J. Fluid Mech., 23, 129-144 (1965).

6. Shmidt, R. J. and Milverson, S. W., "On the Stability of a Fluid when Heated from Below," Proc. Roy. Soc. London, A, 152, 586 (1935).

7. Malkus, W. V. R., "Discrete Transitions in Turbulent Convection," Proc. Roy. Soc. A. 225, 185 (1954).

8. Krishnamurit, R., "On the Transition to Turbulent Convection, Part 1. The Transition from Two to Three-Dimensional Flow," J. Fluid Mech., 42, 2, 295 (1970).

9. Rossby, H. T., "A Study of Benard Convection with and Without Rotation," J. Fluid Mech., 36, 309, (1969).

10. Gaskell, T. F., "The Earth's Mantle," Academic Press, New York, (1967).

11. Bethe, H. A., "Energy Production in Stars," Science, 161, 541, August (1968).

12. Sparrow, E. M., Goldstein, R. J. and Jonsson, V. K., "Thermal Instability in a Horizontal Fluid Layer; Effect of Boundary Conditions and Nonlinear Temperature Profile," J. Fluid Mech. 18, 4, 513 (1964).

→ 13. Roberts, P. H., "Convection in Horizontal Layers with Internal Heat Generation Theory," J. Fluid Mech., 30, L, 33.

14. Thrilby, R., "Convection in an Internally Heated Layer," J. Fluid Mech. 44, 4, 673 (1970).

15. Tritton, D. J and Zarraga, M. N., "Convection in Horizontal Layers with Heat Generation Experiments." J. Fluid Mech. 30, 1, 21 (1967).

16. Joseph, D. D. and Shir, C. C., "Subcritical Convective Instability, Part K, Fluid Layers," J. Fluid Mech., 26, 4, 753 (1966).

→ 17. Horton, C. W. and Rogers, F. T., "Convection Currents in a Porous Medium," J. Applied Phys. 16, 367 (1945).

18. Lapwood, E. R., "Convection of Fluid in a Porous Medium," Prdc. Camb. Phil. Soc., 44, 508 (1948)

19. Lorentzen, G. and Brendeng, E., "On the Influence of Free Convection in Insulated, Vertical Walls," 10th Int. Cong. of Refrigeration, 294 (1959).

→ 20. Martin, G. and Haselden, G. G., "Heat Transfer by Natural Convection in Porous Insulations," 11th Int. Cong. of Refrigeration, Paper 11-2, Munich (1960).

21. Neal, G. and Nader, W., "Practical Significance of Brinkman's Extension of Darcy's Law: Coupled Parallel Flows Within a Channel and a Bounding Porous Medium," The Canadian Journal of Chem. Engg., 52, 475 (1974).

22. List, J., "The Convective Stability of a Confined Saturated Porous Medium Containing Uniformly Distributed Heat Sources," Technical Memorandum, 65-10, CIT (1966).

23. Wooding, R. A., "Steady State Free Thermal Convection of Liquid in a Saturated Permeable Medium." J. Fluid Mech. 2, 273 (1957).

24. Frank, F. C., "On Dilatancy in Relation to Seismic Sources," Rev. Geophs. 3, 485 (1965).

25. Elder, J. W., "Penetrative Convection Its Role in Vulcanism," Bull. Volcan. 29, 327 (1966).

→26. Schneider, K. J. "Investigation of the Influence of Free Thermal Convection on Heat Transfer Through Granular Material," 11th Int. Cong. of Refrigeration, paper 11-4, Munich (1963).

→27. Katto, Y. and Masoka, T., "Criterion for the Onset of Convective Flow in a Fluid in a Porous Medium," Int. J. Heat Mass Transfer, 10, 297-309 (1967).

28. Elder, J. W., "Steady Free Convection in a Porous Medium Heated from Below," J. Fluid Mech., 27, 1, 29 (1967).

→29. Busse, F. and Joseph, D. D., "Bounds for Heat Transport in a Porous Layer," J. Fluid Mech. 54, 521, (1972).

30. Horn, R. N., "Three Dimensional Natural Convection in a Confined Porous Medium Heated from Below," J. Fluid Mech. 92, 751 (1975).

31. Horn, R. N. and O'Sullivan, J. J., "Oscillatory Convection in a Porous Medium Heated from Below," J. Fluid Mech. 66, 339 (1974).

32. Catagirone, J. P., "Thermoconvective Instabilities in a Horizontal Porous Layer," J. Fluid Mech., 72, 169 (1975).

33. Holst, P. H. and Aziz, K., "Transient Three-Dimensional Natural Convection in Confined Porous Media," International J. Heat and Mass Transfer, 15, 73 (1972).

34. Cheng, P. and Teckchandani, L., "Numerical Solution for Transient and Liquid Withdrawal in a Liquid-Dominated Geothermal Reservoir," American Geophys. Union Monograph, 20, 705 (1977).

35. Rana, R., Horne, R. N., and Cheng, P., "Natural Convection in a Multi-Layered Geothermal Reservoir," J. Heat Transfer, 101, 411 (1979).

36. Wilkes, J. O., Ph.D. Thesis, Univ. Michigan, Ann Arbor (1963).

37. Straus, J. M., "Large Amplitude Convection in Porous Media," J. Fluid Mech. 64, 51 (1974).

38. Straus, J. M. and Schubert, G., "Three Dimensional Convection in Cubic Box of Fluid-Saturated Porous Material," J. Fluid Mech., 91, 155 (1979).

39. Joseph, D. D., "Bounds for Heat Transfer in a Porous Layer," Vol. 54, Part 3, 521-543 (1972).

40. Joseph, D. D., "Stability of Convection in Containers of Arbitrary Shape," J. Fluid Mech. 47, 257-282 (1971).

41. Wankat, P. C. and Schowalter, W. R., "Stability of Combined Heat and Mass Transfer in Porous Medium," Phy. Fluid, 13, 2418 (1970).

42. Chow, C. -Y., "An Introduction to Computational Fluid Mechanics," John-Wiley & Sons, New York,(161, 359-374)(1979).

43. Roache, P. J., "Computational Fluid Dynamics," Hermosa Publishers, Albuquerque, N.M. (161, 217, 336) (1972).

44. Torrance, K. E., "Comparison of Finite Difference Computations of Natural Convection," J. of Research of National Bureau of Standards, 728, 281-301 (1968).

45. Torrance, K. E. and Rockett, J. A., "Numerical Study of Natural Convection in an Enclosure with Localized Heating from Below-Creeping Flow to the Onset of Laminar Instability," J. Fluid Mech., 36, 33-54 (1969).

46. Chandrasekhar, S., "Hydrodynamic and Hydromagnetic Stability," Oxford University Press, London, 359-360 (1961).

47. Raley, J. H., Sandholtz, W. A. and Ackerman, F. J., "Results from Simulated, Modified In-Situ Retorting in Pilot Retorts," 11th Oil Shale Symposium Proceedings, CSM. 331 (1978).

48. Lax, P. D. and Richtmyer, R. D., "Survey of the Stability of Linear Finite Difference Equations," Comm. Pure Applied Math. Vol. 9, 267-293, 343-364, (1956).

49. Chapman, A. J., "Heat Transfer: Third Edition, MacMillan Publishing Co., Inc., New York, 576-594, (1974).

CHAPTER VII

APPENDICES

A - Computation of Numerical Stability Criterion:

1. Energy Equation and Navier Stokes Equation:

The energy equation (3.19) can be written in the form:

$$\theta'_{i,j} = a_1\theta_{i+1,j} + a_2\theta_{i-1,j} + a_3\theta_{i,j} + a_4\theta_{i,J+1} + a_5\theta_{i,j-1} \qquad A\text{-}1$$

Lax and Richtmyer (48) showed that the scheme is stable if $a_3 > 0$ in (A-1). From the energy equation, a_3 is the coefficient of $\theta_{i,j}$, which can be calculated as:

$$\theta'_{i,j} = \theta_{i,j} + \frac{\Delta\tau}{2h}\Big[-((Uf-Uf)\theta_{i+1,j}+(Uf+|Uf|-Ub+|Ub|)\theta_{i,j} -(Ub+|Ub|)\theta_{i-1,M})-((Vf-Vf)\theta_{i,j+1} +(Vf+|Vf|-Vb +|Vb|)\theta_{i,j}-(Vb+|Vb|)\theta_{i,j-1})+2/prh (\theta_{i+1,j}+\theta_{i-1,j} +\theta_{i,j-1}-4\,\theta_{i,j})\Big]$$

By collecting the coefficients of $\theta_{i,j}$, equating to zero and rearranging,

$$\Delta\tau \leq (1/2h(Uf+|Uf|- Ub+|Ub|- Vf+|Vf|-Vb+|Vb|)- 4/prh^2)$$

2. Brinkman's Extension of Darcy's Law:

By following the same procedures as used in the energy equation,

$$\Delta\tau \leq \left(\frac{1 - N}{1/2h(Uf+|Uf|- Ub+|Ub|-Vf+|Vf|-Vb+|Vb|-4/prh^2)}\right)$$

B. Physical Properties of Air and Sandstone

B-1. All physical properties of air and sandstone are taken from Reference(49).

B-2. The pressure drop and fluid velocity are taken from Reference (47), they are:

$\Delta p(lb/ft^2)$	0.201	0.204	0.816	20.4
V (ft/sec)	0.033	0.062	0.038	0.038

C. Computer Programs

Four programs are employed in the present work. They will be referred to descriptively as: ASH.For, SAL.For, KAL.For, RAM.For. It must be noted that those programs are modified from Chow (42) original programs, and may be described briefly as follows:

C-1. ASH.For: The main program which calls the other three subroutines. This program specifies the initial and boundary conditions for U, V, θ, and w. It reads the data of variable parameters Gr, Pr, γ, Re, N and maximum steps. It also specifies the grid spacing M, N, at anytime temperature and vorticity distributions are obtained from the conditions at the previous time step.

C-2. SAL.For: It is the subroutine called (SoRLX) which is used to find the stream function for a certain known vorticity distribution by solving the poisson-type equation. The maximum error allowed in this program for the successive relaxation method is .0001. The boundary conditions stated in this subroutine are those stated in Section (3.5-C).

C-3. KAL.For: It is the subroutine contour which is used for the purpose of plotting the flow by printing different symbols in the fluid domain, depending on the local values of the stream functions and the temperature. The final output shows a rough picture of the flow pattern or of the iso-thermals depending on the contour plot required to be seen. Flow patterns or/and iso-thermals are plotted only at particular time steps when the number of steps equals one of the selected values stored in the array NPLOT in the main program.

Computer output will show the following symbols corresponding to the following data values. (Figs.4.12-4.27)

1- Stream Function

A	For	$\psi \leq -2.0$
B	"	$-0.5 \leq \psi \leq -0.3$
C	"	$-0.2 \leq \psi \leq -0.05$
D	"	$-0.01 \leq \psi \leq -0.003$
-	"	$-0.001 \leq \psi \leq 0.0$
+	"	$0.0 \leq \psi \leq 0.001$
1	"	$0.003 \leq \psi \leq 0.01$
2	"	$0.05 \leq \psi \leq 0.2$
3	"	$0.3 \leq \psi \leq 0.5$
4	"	$0.6 \leq \psi \leq 0.7$
5	"	$0.8 \leq \psi \leq 0.9$
6	"	$1.0 \leq \psi \leq 2.0$

2. Temperature

+	For	$0.0 \leq \theta \leq 0.001$
1	"	$0.003 \leq \theta \leq 0.01$
2	"	$0.05 \leq \theta \leq 0.2$
3	"	$0.3 \leq \theta \leq 0.5$
4	"	$0.6 \leq \theta \leq 0.7$
5	"	$0.8 \leq \theta \leq 0.9$
6	"	$\theta > 1.0$

C-4. RAM.For: It is the function PNEW which is used to comput the vorticity and temperature at all interior points except those on the center line along which the vorticity vanishes. This is just the integration by finite difference of the energy and vorticity equations. For Darcy's Law the vorticity is calculated in the main porgram using equation (3.18).

It must be noted that all three programs, except (SAL.For) are changed from run to run according to the change in the aspect ratio "where M and N are changed", or according to the expression of the vorticity equation whether it is according to Navier, Brinkman's or Darcy's Law. For Navier Stokes and Brinkman's Darcy's the function PNEW is used to integrate both the energy and the vorticity equations.

The program listing presented here is just for one case run and it has to change some of its statements according to the run requirement as stated earlier.

```
C-------------------------------------------------------
C********PROGRAM (ASH.FOR),INSTABILITY OF FLUID
C*******FLOW THROUGH POROUS MEDIA HEATED FROM BELOW*****
C-------------------------------------------------------
      DIMENSION PSI(10,10),U(10,10),V(10,10),OMEGA(10,10)
     1,OMNEW(10,10),THNEW(10,10),RHS(10,10),NPLOT(10),
     1THETA(10,10)
      COMMON H,DT,I,J,UF,UFA,UB,UBA,VF,VFA,VB,VBA
      WRITE(4,105)
C********FAC IS THE RATIO OF HEAT CAPACITY DENSITY OF THE
C*******FLUID TO THAT OF THE MEDIUM ITS VALUE IS EQUAL
C***** TO 4.E-4 FOR POROUS MEDIA AND 1.E00 FOR
C***** SINGLE PHASE  ******************************
105   FORMAT(5X,'WHAT IS GR,DT,FAC, RE,PR,RN,MAXSTP')
      READ(4,106) GR,DT,FAC,RE,PR,RN,MAXSTP
106   FORMAT(6E,I)
      DATA NPLOT/10,50,100,200,300,400,500,600,700,800/
      PRINVS=FAC/PR
      M=10
      MM1=M-1
      N=10
      NM1=N-1
      RATIO=MM1/NM1
      H=1./(N-1.)
C******** SPECIFY INITIAL CONDITIONS FOR U,V,OMEGA,THETA.
C******* OMEGA AND U WILL BE KEPT THE SAME FOR ALL TIMES ****
      NSTEP=0
      NFIG=0
      T=0.0
      DO 1 I=1,M
      DO 1 J=1,N
      U(I,J)=0.0
      V(I,J)=RE
      OMEGA(I,J)=0.0
      THETA(I,J)=0.0
1     IF(J.EQ.1) THETA(I,J)=1.
C*****  COMPUT STREAM FUNCTION BASED ON VORTICITY FIELD *****
2     DO 3 I=1,M
      DO 3 J=1,N
3     RHS(I,J)=-OMEGA(I,J)
      CALL SORLX(PSI,RHS,M,N,H,.0001,ITER,RE)
C*****  COMPUTE U,V AT INTERIOR POINTS *****
      DO 4 I=2,MM1
      DO 4 J=2,NM1
      U(I,J)=(PSI(I,J+1)-PSI(I,J-1))/(2.*H)
4     V(I,J)=-(PSI(I+1,J)-PSI(I-1,J))/(2.*H)
      DO 5 J=2,NM1
5     V(M,J)=PSI(MM1,J)/H
C***** COMPUTE VORTICITY AND STREAM FUNCTIONS AT INTERIOR GRID****
C***** POINTS . COMPUTATION WILL BE TERMENATED IF NSTEP EXCEEDS***
C***** (MAXSTP). INCREASE TIME STEP BY ONE                      ***
```

```
      NSTEP=NSTEP+1
      IF(NSTEP.GT.MAXSTP) STOP
      T=T+DT
      DO 6 I=2,MM1
      DO 6 J=2,NM1
      UF=(U(I+1,J)+U(I,J))/2.
      UFA=ABS(UF)
      UB=(U(I-1,J)+U(I,J))/2.
      UBA=ABS(UB)
      VF=(V(I,J+1)+V(I,J))/2.
      VFA=ABS(VF)
      VB=(V(I,J-1)+V(I,J))/2.
      VBA=ABS(VB)
      THNEW(I,J)=PNEW(THETA,THETA,M,N,FAC,0.0,PRINVS,0.0)
C***** THE NEXT STATEMENT IS USED ONLY WHEN THE VORTICITY
C**** EQUATION EXPRESSED BY BRINKMAN EXTENSION OF DARCY'S
C**** LOW OR BY NAVIER STOCK EQUATION (RN=0.0). **************
C     OMNEW(I,J)=PNEW(OMEGA,THETA,M,N,0.0,GR,0.0,RN)
C***** THE NEXT STATEMENT IS USED WHEN THE VORTICITY EQN.
C***** IS EXPRESSED BY DARCY'S LAW                          ****
6     OMNEW(I,J)=GR/(RN*2.*H)*(THETA(I+1,J)-THETA(I-1,J))
      DO 7 J=2,NM1
      UB=U(M-1,J)/2.
      UBA=ABS(UB)
      UF=(U(2,J)+U(1,J))/2.
      UFA=ABS(UF)
      VF=(V(M,J+1)+V(M,J))/2.
      VF1=(V(1,J+1)+V(1,J))/2.
      VFA=ABS(VF)
      VF1A=ABS(VF1)
      VB=(V(M,J-1)+V(M,J))/2.
      VB1=(V(1,J-1)+V(1,J))/2.
      VBA=ABS(VB)
      VB1A=ABS(VB1)
      P1=-2.*(UB+UBA)*THETA(MM1,J)+2.*(-UB+UBA)*THETA(M,J)
      P11=2.*(UF-UFA)*THETA(2,J)+2.*(UF+UFA)*THETA(1,J)
      P2=(VF-VFA)*THETA(M,J+1)+(VF+VFA-VB+VBA)*THETA(M,J)
     1-(VB+VBA)*THETA(M,J-1)
      P22=(VF1-VF1A)*THETA(1,J+1)+(VF1+VF1A-VB1+VB1A)*THETA(1,J)
     1-(VB1+VB1A)*THETA(1,J-1)
      P4=2.*THETA(MM1,J)+THETA(M,J+1)+THETA(M,J-1)-4.*THETA(M,J)
      P44=2.*THETA(2,J)+THETA(1,J+1)+THETA(1,J-1)-4.*THETA(1,J)
C***** CALCULATION OF NUMERICAL INSTABILITY CRITERION **********
      P5=1./(2.*H)*(UF+ABS(UF)-UB+ABS(UB))
      P6=1./(2.*H)*(VF+ABS(VF)-VB+ABS(VB))
C***** RN IS EQUAL 0.0 WHEN THE NEXT STATEMENT IS USED
C***** FOR THE ENERGY EQUATION OR NAVIER STOKES EQN.,
C***** AND USED AS IT IS WHEN BRINKMAN EXT. OF DARCY'S
C***** LAW IS USED                                          ****
      P7=(1.-RN)/(P5+P6+4.*PRINVS/(H*H))
      THNEW(M,J)=THETA(M,J)+DT/(2.*H)*((-P1-P2)*FAC+2.*PRINVS*P4/H)
```

```
      THNEW(1,J)=THETA(1,J)+DT/(2.*H)*((-P11-P22)*FAC+2.*PRINVS*P44/H)
7     OMNEW(M,J)=0.0
C*****  THE ELEMENTS OF OMNEW ,THNEW ARE ASSIGNED TO OMEGA ,AND THETA***
      DO 8 I=2,M
      DO 8 J=2,NM1
      OMEGA(I,J)=OMNEW(I,J)
8     THETA(I,J)=THNEW(I,J)
C***** OMEGA AT THE BOUNDARIES ARE UPDATED       **********************
      DO 9 I=2,MM1
      OMEGA(I,1)=(-4.*U(I,2)+U(I,3))/(2.*H)
9     OMEGA(I,N)=(4.*U(I,N-1)-U(I,N-2))/(2.*H)
      DO 10 J=2,NM1
      IF(THETA(1,J).EQ.0.0) THETA(1,J)=THETA(M,J)
10    OMEGA(1,J)=(4.*V(2,J)-V(3,J)-3.*V(1,J))/(2.*H)
C***** DEPENDING ON THE NEXT 'CALL' ,PLOT ISOTHERMALS
C***** OR STREAM LINES WHEN NSTEP EQUALS ONE OF THE
C***** VALUES SPECIFIED IN 'NPLOT'                    *******
      DO 11 K=1,10
      IF(NSTEP-NPLOT(K))11,12,11
11    CONTINUE
      GO TO 2
12    NFIG=NFIG+1
      WRITE(3,13)
13    FORMAT(1H1)
14    WRITE(3,15)
15    FORMAT(//)
      CALL CONTUR(PSI,1.,1.0,70,H)
      WRITE(3,25) T,GR,RN,PR,RE,P7,RATIO,NSTEP,MAXSTP
25    FORMAT(//51X,'TIME=',E/51X,'GR=',E/51X,'RN=',E/
     151X,'PR=',E/51X,'RE=',E/51X,'P7=',E/51X,
     1'RATIO=',E/51X,'NSTEP=',I/51X,'MAXSTP=',I)
      GO TO 2
      END
```

```
      SUBROUTINE SORLX(F,Q,M,N,H,ERRMAX,ITER,RE)
C-------------------------------------------------------
C***** PROGRAM 'SAL.FOR' ,SUCCESSIVE OVERRELAXATION
C***** METHOD TO SOLVE POISSON TYPE EQUATION OF THE FORM
C***** LAP(F)=Q IN A RECTANGULAR DOMAIN       *******
C-------------------------------------------------------
      DIMENSION F(M,N),Q(M,N)
      MM1=M-1
      NM1=N-1
C*****  CALCULATE THE OPTIMUM VALUE OF OMEGA *************
      PI=4.*ATAN(1.)
      ALPHA=COS(PI/M)+COS(PI/N)
      OPTOM=(8.-4.*SQRT(4.-ALPHA**2))/ALPHA**2
C***** INITIAL AND BOUNDARY CONDITIONS FOR STREAM FUNCTION ****
      ITER=0
      DO 1 I=1,M
      DO 1 J=1,N
1     F(I,J)=H*RE*(I-M)
C*****  BEFORE EACH ITERATION ADD ONE  TO ITER*****
2     ITER=ITER+1
      ERROR=0.0
C*****  COMPUTE F(I,J) AT ENTERIOR POINTS*****
      DO 3 I=2,MM1
      DO 3 J=2,NM1
      FOLD=F(I,J)
      F(I,J)=F(I,J)+.25*OPTOM*(F(I-1,J)+F(I+1,J)+F(I,J-1)
     1+F(I,J+1)-4.*F(I,J)-H*H*Q(I,J))
3     ERROR=ERROR+ABS(F(I,J)-FOLD)
      IF(ERROR.GT.ERRMAX) GO TO 2
      RETURN
      END
```

```
      SUBROUTINE CONTUR(PSI,XRANGE,YRANGE,NX,H)
C-------------------------------------------------------
C***** PROGRAM 'KAL.FOR' , CONTUR PLOT FOR PSI OR THETA
C***** IN RECTANGULAR DOMAIN OF SIZE (XRANGE)*(YRANGE)
C***** NX IS THE NUMBER OF SYMBOLS TO BE PRINTED IN
C***** A HORIZONTAL LINE, AND H IS THE SQUARE GRID SIZE
C***** BASED ON WHICH VALUES OF PSI(I,J) OR THETA(I,J)
C***** ARE PLOTTED. SYMBOLS SPECIFIED IN ARRAY 'SYMBOL'
C***** ARE THOSE USED FOR 'PSI' OR 'THETA' FALLING WITHIN
C***** THE INTERIOR BOUNDED BY VALUES SPECIFIED IN THE
C***** ARRAY 'VALUE'                                  ***
C-------------------------------------------------------
      REAL LX,LY
      DIMENSION PSI(10,10),VALUE(22),SYMBOL(23),GRAPH(100)
      DATA VALUE/-2.,-.5,-.3,-.2,-.05,-.01,-.003,-.001
     1,.0,.001,.003,.01,.05,.2,.3,.5,.6,.7,.8,.9,1.,2./
      DATA SYMBOL/1HA,1H ,1HB,1H ,1HC,1H ,1HD,1H ,1H-,
     11H+,1H ,1H1,1H ,1H2,1H ,1H3,1H ,1H4,1H ,1H5,1H ,1H6,1H /
      NY=.6*NX*YRANGE/XRANGE
      DELX=XRANGE/NX
      DELY=YRANGE/NY
      DO 5 JSYMBL=1,NY
      Y=YRANGE-(JSYMBL-.5)*DELY
      J=1+Y/H
      LY=Y-(J-1)*H
      HMLY=H-LY
      DO 4 ISYMBL=1,NX
      X=(ISYMBL-.5)*DELX
      I=1+X/H
      LX=X-(I-1)*H
      HMLX=H-LX
      A1=HMLX*HMLY
      A2=HMLX*LY
      A3=LX*LY
      A4=LX*HMLY
      PSIC=(A1*PSI(I,J)+A2*PSI(I,J+1)+A3*PSI(I+1,J+1)+
     1A4*PSI(I+1,J))/H**2
      DO 2 K=1,22
      IF(PSIC-VALUE(K))1,1,2
1     NRANGE=K
      GO TO 3
2     CONTINUE
      NRANGE=23
3     GRAPH(ISYMBL)=SYMBOL(NRANGE)
4     CONTINUE
5     WRITE(3,6)(GRAPH(I),I=1,NX)
6     FORMAT(20X,100A1)
      RETURN
      END
```

```
C***** PROGRAM 'RAM.FOR',TO INTEGRATE EQUATION OF THE
C***** FORM DP/DT=-D(UP)/DX-D(VP)/DY+A*DQ/DX+B*LAP(P)
C***** IN WHICH D AND LAP REPRESENT PARTIAL DERIVATIVE
C***** AND LAPLACIAN OPERATORS RESPECTIVELY          *****
      FUNCTION PNEW(P,Q,M,N,FAC,A,B,C)
      DIMENSION P(M,N),Q(M,N)
      COMMON H,DT,I,J,UF,UFA,UB,UBA,VF,VFA,VB,VBA
      P1=(UF-UFA)*P(I+1,J)+(UF+UFA-UB+UBA)*P(I,J)
     1-(UB+UBA)*P(I-1,J)
      P2=(VF-VFA)*P(I,J+1)+(VF+VFA-VB+VBA)*P(I,J)
     1-(VB+VBA)*P(I,J-1)
      P3=Q(I+1,J)-Q(I-1,J)
      P4=P(I+1,J)+P(I-1,J)+P(I,J+1)+P(I,J-1)-4.*P(I,J)
      PNEW=P(I,J)+DT/(2.*H)*((-P1-P2)*FAC+A*P3+2.*B*P4/H)
     1-C*P(I,J)
      RETURN
      END
```